JCIM JOURNAL OF CHEMICAL INFORMATION AND MODELING

pubs.acs.org/jcim Review

Current Trends in Computational Quantum Chemistry Studies on Antioxidant Radical Scavenging Activity

Maciej Spiegel*

Cite This: J. Chem. Inf. Model. 2022, 62, 2639−2658 Read Online

ACCESS | Metrics & More | Article Recommendations

ABSTRACT: The antioxidative nature of chemicals is now routinely studied using computational quantum chemistry. Scientists are constantly proposing new approaches to investigate those methods, and the subject is evolving at a rapid pace. The goal of this review is to collect, consolidate, and present current trends in a clear, methodical, and reference-rich manner. This paper is divided into several sections, each of which corresponds to a different stage of elaborations: preliminary concerns, electronic structure analysis, and general reactivity (thermochemistry and kinetics). The sections are further subdivided based on methodologies used. Concluding remarks and future perspectives are presented based on the remaining elements.

KEYWORDS: *Antioxidants, density functional theory, computational chemistry, electronic structure, weak interactions, kinetics, thermochemistry, QM-ORSA*

INTRODUCTION

Free radicals play a crucial role in the maintenance of homeostasis by participating in a range of physiologically relevant processes such as immune response and intracellular communication. Nonetheless, whatever the case may be, their uncontrolled accumulation is not favorable. The energy they possess as a due to the unpaired electron on the valence shell or excited state cannot be efficiently neutralized by intracellular antioxidant defense system and is instead transferred to the biologically important targets like lipids, carbohydrates, proteins, and DNA strains. In consequence, these structures degenerate, leading to the development of severe malfunctions resulting in illness such as diabetes, atherosclerosis, Alzheimer's and Parkinson's diseases, or tumor growth.[1,2]

The expanding awareness of the dual nature of radicals has prompted a surge in interest in compounds that can decrease elevated levels of reactive oxygen, nitrogen, and sulfur species, thereby preventing their harmful activity. These substances, known as *antioxidants*, are a heterogeneous group of molecules able to reduce oxidative stress in different ways. They are classified as follows[3]

- Type I: chain breakers, which interact directly with radicals by creating species that are more stable and less hazardous to cells than the former ones, thus terminating chain reactions and preventing oxidation of biological targets.
- Type II: preventers, for which, however, a unified mechanism of action is not specified, but it does not include interactions with radicals. Among known activities of that type are metal chelation, particularly iron and copper, which participate in the Fenton reaction, as well as regulation of enzymes responsible for radical formation or those directly involved in oxidative stress development.[1,2,4] Compounds capable of regenerating biological antioxidants[1] or absorbing UV radiation[5] are also included in this category.
- Type III: substances that effectively repair oxidatively damaged biomolecules.[1]

However, because most antioxidants exhibit multiple types of activity at the same time, such categorization is often artificial. It is better to do so on the basis of their chemical structure or origin.

Phytochemicals are plant-derived compounds that are plentiful in many herbs and commonly consumed plants such as beetroot, high in betalains;[6] tea, rich in catechins;[7] or grapefruit, abundant in flavanons.[8] This family can be further subdivided into flavonoids,[9,10,19−28,11,29−37,12−18] phenolic acids,[38−47] lignans,[48] aurones,[49] chalcones,[49−51] curcuminoids,[52,53] anthocyanidins,[54−56] stilbenoids;[28,57−59] anthraquinones,[60−63] glucosinolates,[64,65] alkaloids,[66,67] coumarins,[68] terpenes and terpenoids,[68−72] and others[41,73,82−86,74−81] (Figure 1), all of them being extensively studied with computational quantum chemistry methods, as evidenced by the number of recent scientific findings. Albeit, plants are not the

Received: January 25, 2022
Published: April 18, 2022

https://doi.org/10.1021/acs.jcim.2c00104
J. Chem. Inf. Model. 2022, 62, 2639−2658

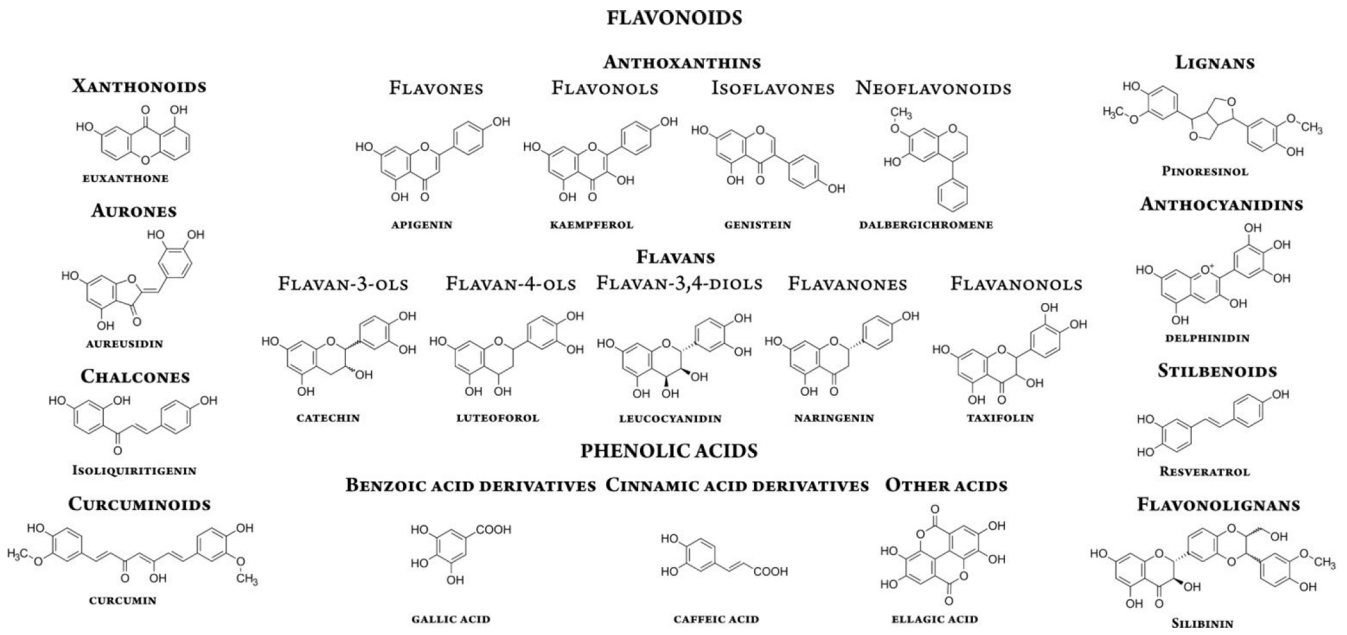

Figure 1. Some of the most commonly distinguished subtypes of dietary antioxidants and their representative examples.

only source of antioxidants —substances with promising antiradical activities have also been found among common drugs,[87−92] biological substances,[93−102] and their metabolites.[59,93,98,100,103−105] All of the listed substances are being heavily modified in an effort to identify derivatives with an improved safety profile and enhanced radical scavenging potential.[23,36,102,106−114,46,115−124,83,125,86,87,89,94,96,101]

Finally, completely novel structures are proposed and investigated on the basis of recognized pharmacophores: phenolic units,[126−132] five-heterocyclic rings,[133−139] quinoline backbones,[140−142] and other moieties.[143−146] Importantly, despite their diversity, chain breakers share similar reactivity patterns and mechanisms, allowing common theoretical approaches to be used to study any of them.

This review outlines currents trends in "Type I" activity research in a straightforward and methodical manner. The first section deals with preliminary concerns, such as selecting the appropriate level of theory, the solvation model, and the initial structures. Following that, the topic of electronic structure examination is discussed in light of the methodologies documented in the literature. The majority of this work is devoted to thermochemistry and kinetics research, which are the most important for comparing computationally produced results with experimental data. Finally, remaining issues are highlighted and perspectives on the subject provided.

Before proceeding, it is important to note that while this review specifically mentions hydroxyl groups any other residue in which a hydrogen atom is bonded to a highly electronegative atom, such as nitrogen in an amino group or sulfur in a thiol group, can also be considered as the one that may participate in antioxidative activity.[46]

PRELIMINARY CONCERNS

The level of theory chosen, which describes the electronic structure of the molecule *as itself*, and the solvation model, which adjusts the system's electron density cloud to minor perturbations caused by solvent molecules, are two key components influencing chemical behavior that must be taken into account from the beginning of the studies.

Functional and Basis Set. It is frequently advantageous to obtain results that precisely resemble experimental data while needing the least amount of computational time. However, this seemingly easy task is burdened with two fundamental issues: (1) With so many functionals and basis sets available, choosing a level of theory satisfying this condition is difficult. (2) The lack of reference data against which theoretical findings may be compared casts doubt on the latter. Although high-end methods such as CCSD(T)/CBS guarantee quality of the outcomes, this solution is inapplicable for routine computations due to the significant uptake of resources.

As shown in Chart 1, there is currently a trend toward the use of density functional theory (DFT) methods, with B3LYP[147,148]

Chart 1. Share of Functionals in Articles Published in the Last Five Years[a]

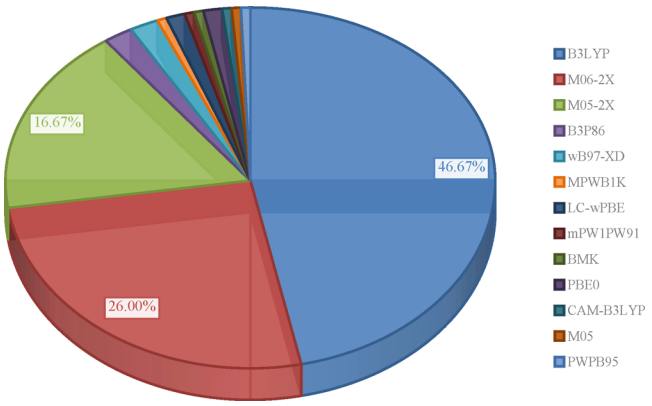

[a]Plotted on the basis of refs 9−146.

(∼47%), M06-2X[149] (∼26%), and M05-2X[150] (∼17%) being picked the most commonly. Restricting to any of them is advantageous because it provides researcher a plethora of datapoints the comparison with validate the results in a greater degree than it would happen if was done against outcomes obtained by completely differently constructed functional.

https://doi.org/10.1021/acs.jcim.2c00104
J. Chem. Inf. Model. 2022, 62, 2639−2658

Moreover, other researchers following the given reasoning would more likely cite the paper that use common level of theory since it enables to compare their own theoretical results with those provided by other researchers.

Given their newness, it is visible that these two Minnesota functionals are gradually displacing B3LYP since their release. This could be a result of their superior performance in estimating thermochemistry, kinetic and noncovalent interactions of nonmetal elements, as well as energies of reactions involving free radicals, which they predict extremely close to actual data, as claimed by the developers[149−151] and continue to be substantiated by independent scientists, either in the course of original research[39−41,45,77,84,87,129] or in benchmarks.[152−154] On the other hand, several researchers who used both B3LYP and one of Truhlar's global hybrids noted that while B3LYP tends to underestimate energies there are no substantial differences and the reactivity patterns hold when the same basis set is used.[60,64,95,123,127]

Although the reasons for selecting certain functional are usually covered in the manuscript with details, the arguments for choosing "*this, but not that*" basis set are nearly always glossed over. This bad habit have its consequences in the performance of computations. Increasing the number of basis functions is known to increase task processing time, and it has recently been established that those from the Dunning's and Ahlrich's families are particulary vulnerable.[153] Furthermore, whereas functionals should be kept constant throughout the research, the basis set does not, namely while one can be used for electronic structure investigations, other may be applied for thermochemistry, which allows maneuvering them in order to obtain the best results at the lowest possible cost.

As a result, Chart 2, which depicts the percentage of basis sets used for thermochemistry computations, is much more divided

Chart 2. Share of Basis Sets in Articles Published in the Last Five Years[a]

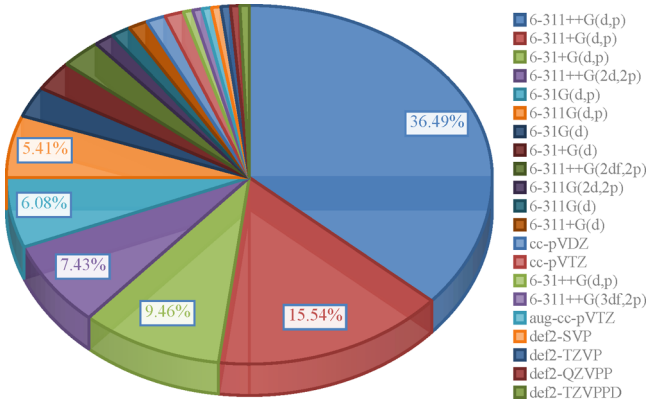

[a]Plotted on the basis of refs 9−146.

than the previous one, with Pople's leading the way. A particularly good observation is that combining any of them with one of the three most commonly employed functionals presented in Chart 1, appears to have a little influence on the results as evidenced in the following examples. The findings of Shammera Ahamed et al.[79] (B3LYP and M062X combined with either 6-31+G(d,p) or 6-311++G(d,p)) and Mendes et al.[12] (B3LYP, LC-wPBE, M062X, and BMK in 6-311G(d,p) and 6-311+G(d,p) bases) show that despite the augmentation of basis set with another diffuse function or inclusion of next function describing valence shell, the values of reactivity indices found in the gas phase change only slightly, regardless of level of theory used. In their other study,[26] the authors demonstrated that shifting from 6-311G(d,p) to 6-311+G(d,p) changed the ionization potential values by less than 4 kcal/mol independently of the environment (gas phase, water, methanol, ethanol, *n*-hexane). Similar results were observed in the investigations of Bakir et al.[146] (B3LYP/6-31G(d,p) and B3LYP/6-311++G(2d,2p)) and Santos et al.[60] (B3LYP/6-31+G(d,p), B3LYP/6-31++G(d,p) and B3LYP/6-311+G(d,p)), both of which were conducted in gas and water. On the other hand, the differences in ionization potential and electron transfer energy associated with ion formation in water milieu were found to be significantly smaller in the case of B3LYP/6-311++G(d,p) outcomes when compared to those obtained at B3LYP/6-31+G(d,p) level of theory.[79]

Moreover, although the presence of polarization functions is undeniably important for determining the energy of highly polarized bonds, the role diffusion functions, which are widely regarded as necessary for accurately modeling electron clouds in ionic systems and radical involving pathways, must be addressed more thoroughly. Still, the recent research[153] has shed new light on that issue for it was discovered that using 6-311G(d,p) for overall antioxidant studies produces the best results in terms of both the accuracy between theroetical outcomes and experimental values, as well as computational resource uptake. Further confirmation on that indulging issue and more detailed studies on the role of the basis set are welcome.

It is worth noting that open shell computations are hampered by the possibility of spin contamination.[155] This is because the resulting wave function is an artificial mix of spin states rather than an eigenfunction of total spin, $\langle S^2 \rangle$. In an ideal system, $\langle S^2 \rangle$ equals 0.75 for singlet and 2.0 for triplet

$$\langle S^2 \rangle = s(s+1) \tag{1}$$

where s denotes the number of unpaired electrons divided by half. Other values are acceptable as long as they deviate by no more than 10%.[10,109,152] Greater ones indicate the presence of higher spin states, which may alter the energy or geometry, just like the population analysis outcomes, resulting in biased conclusions; such structures should not be considered for future research. Spin-restricted open shell computations may be a solution in those cases, but they consume more resources than unrestricted ones and may still produce incorrect energies of unpaired electrons due to the absence of dynamical correlation caused by the vanishing of spin polarization.

Solvation Model. The physiological media in which antioxidants play fundamental biological roles are body fluids and the lipid bilayer of cells membrane. As a consequence, most experiments are conducted in water or in a nonpolar environment, that computational elaborations must account for. The effect of a polar solvent is a fundamental tenet of theoretical investigations because it distorts a molecule's electron cloud due to electrostatic polarization interactions, affecting the shape of the potential energy surface and chemical activity.[3,20,28,130,156] Furthermore, if the reaction pathway involves proton or electron detachment, the solvation is a known to be a driving force that eases the process and makes it more feasible than it would be in a nonpolar medium.[50,116] That is why it is also important for properly modeling dissociation related processes as is stressed later in the text.

For the time being, three methods are employed to incorporate solvent effects: implicit (through a homogeneously

https://doi.org/10.1021/acs.jcim.2c00104
J. Chem. Inf. Model. 2022, 62, 2639−2658

polarizable medium), explicit (by solvent molecules), and a combination of these two. The integral equation formalism variation of the polarizable continuum model (IEFPCM, often referred to as just PCM),[157] conductor-like polarizable continuum model (CPCM),[158,159] and solvation model based on density (SMD)[160] are examples of continous solvation models that are implemented in a majority of quantum chemistry software. They are also the most frequently used because they are burdened with a much lower computing cost than implicit or combined approach.

However, the fundamental disadvantage of implicit models is complete negation of intermolecular hydrogen bonds, which are often essential for proper simulation of antiradical activity[93,103,144] especially when abundant as in the case of capsaicin.[84] A mutual competition between intramolecular and intermolecular hydrogen bonds is also observed as a relevant factor modying hydrogen atom transfer proclivity.[47] The modeling of $^{\bullet}$OH and $^{\bullet}$OOH radicals, which are of primary interest in antioxidants research, is an excellent example of how the explicit water molecules can influence the results as well. Accordingly to Pérez-González and Galano,[125] adding the first water molecule considerably changed the rate constants of the $^{\bullet}$OH/$^{-}$OH path, but adding more or repeating the procedure for the $^{\bullet}$OOH/$^{-}$OOH path resulted in no significant change. The fact that their charge is concentrated on a single exposed heteroatom[161] is important here.

The application of a homogeneously polarizable medium is a particularly viable method of modeling solvents having large structures. For example, representing the enormous membrane lipid chains would be a time-consuming and inefficient effort. Instead, one of the most common approaches found in the literature is to do that implicitly, by using the largest available aprotic solute, for example, pentyl ethanoate.[12,100,107,120,132] To account for the cage effect, which manifests as the loss of entropy of any chemical reaction with a molecularity of two or greater, and improve results, the Okuno's corrections[162] and Benson's free volume theory[163] can be applied (eq 2), as demonstrated.[40,41,104] The corrected Gibbs free energy, ΔG^{FV}_{solv}, is expressed then in a form of

$$\Delta G^{FV}_{solv} = \Delta G^{0}_{solv} - RT\{\ln[n10^{(2n-2)}] - (n-1)\} \quad (2)$$

where n represents the molecularity of the reaction, and ΔG^{v0}_{sol} is a Gibbs free energy in solvent, R a gaseous constant, and T the temperature[164]

Initial Structure. Let's refere a thorough conformational studies[156,165] that were performed on a collection of quercetin structures with variable planarity and intramolecular hydrogen bond counts. These two structural features are known to account for antioxidative activity of flavonoids, and so considerable differences have been found among them. This is not the only case, for similar geometry−activity relationships have been pinpointed also in other studies.[60,91,107,134] This emphasizes the role of selecting the appropriate conformer for the study as a critical first step in theoretical elaborations.

Molecular dynamics (MD) simulations are most effective for producing excellent starting structures. Different approaches can be undertaken to run MD calculations, such as using software that has implemented molecular mechanic potentials and thus allows for the direct conformational search procedure[166−168] or dedicated ones designed for more demanding studies, like GROMACS,[169] Amber,[170] or CHARMM,[171] for which the molecule under consideration must first be parametrized. This can be done with either the proposed protocols[84] or available webservices the most well recognized of which is probably CharmmGUI,[172] although AutomatedTopologyBuilder (ATB)[173] should also be mentioned.

CharmmGUI has an advantage over ATB in that it has a user-friendly interface and instantly generates a complete set of files that can be submitted for molecular dynamics, whereas ATB only produces force field, structure, and topology data, leaving the user to prepare the remaining files. CharmmGUI, on the other hand, predicts topology using CGenFF,[174] which elucidates it through bond perception and atom typing, while ATB processes input using DFT or semiempirical techniques depending on the size of the system. After all, it is the user's expertise that determines which path to take.

MD frequently generates a large number of molecules, whilst upcoming quantum chemical studies should only consider the most populated states. One of the first filters used to get rid of the undesired structures is the geometric clustering algorithm[175] which, in simple terms, groups conformers based on their structure or kinetics. If there are multiples of them, optimization at the appropriate level of theory followed by Maxwell−Boltzmann distribution analysis may be a viable approach for removing superfluous structures, particularly those with molar fractions less than 0.1%. This threshold is proposed[46,101,112] because a small energy difference between conformers could indicate an interconversion process: rotatability of OH groups[165] or side chains,[84] bonds deformation due to keto−enol tautomery,[21] shift in E/Z-conformers equilibria,[133] and bending of dihedral angles.[16,20,28,33,50,67,128,165] They can all modulate hydrogen bonds, electrons cloud delocalization, and polarizability, as well as radical accessibility to specific sites of an antioxidant. Furthermore, the molar fraction cannot be too low if the compound is desired to pass biological barriers.[46]

Two equations (eqs 3 and 4) can be used to evaluate the Maxwell−Boltzmann population f of a specific conformer i, in the set of n conformers

$$f_i = \frac{\exp\left(\frac{-G_{i(aq)}}{RT}\right)}{\sum_{i=1}^{n}\exp\left(\frac{-G_{i(aq)}}{RT}\right)} \text{ for } i = 1, 2, \cdots, n \quad (3)$$

and

$$\sum_{i=1}^{n} f_i = 1 \quad (4)$$

where R is the gas constant, and T is the temperature. $G_{i(aq)}$, the aqueous phase Gibbs free energy of the ith conformer, can be calculated following eq 5

$$G_{i(aq)} = G_i^{\circ} + \Delta G^{1atm\rightarrow 1M} + \Delta G_i^{*} \quad (5)$$

where G_i° denotes a species' gas phase free energy at a given temperature, $\Delta G^{1atm\rightarrow 1M} = 1.89$ kcal/mol and reflects the shift in standard state from 1 atm (superscripted with $^{\circ}$) to 1 M (superscripted with $*$), and ΔG_i^{*} denotes a species' aqueous solvation free energy.

Deprotonation and Dissociation Constants. The primary activity of type I antioxidants is based on their reductant capacity, which is frequently, but not always[64,68,125] linked to the hydrogen-donation capacity from one of their aromatic hydroxyl groups; thus, a simple conclusion can be drawn that the more of them, the greater shall be participation of hydrogen-related channels in overall radical scavenging, and so its viablity.[116]

https://doi.org/10.1021/acs.jcim.2c00104
J. Chem. Inf. Model. 2022, 62, 2639−2658

Scheme 1. Various Thermodynamic Cycles Used to Calculate the Free Energy of Deprotonation

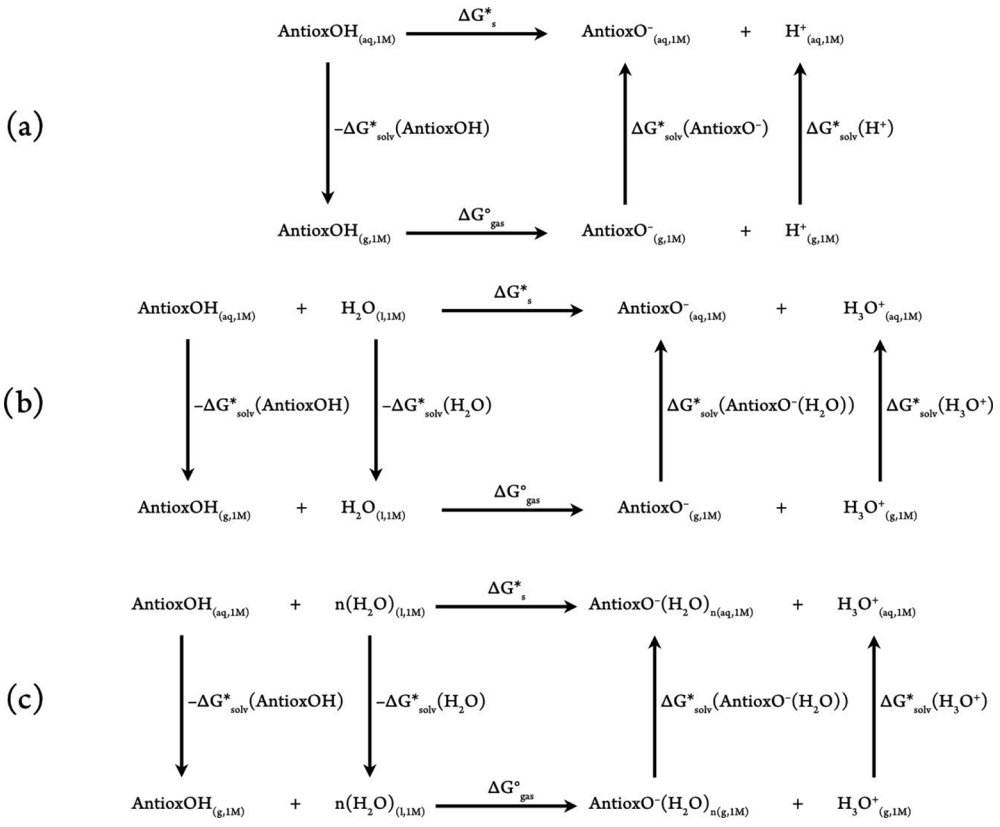

However, because these residues are also weakly acidic, multiple species can coexist in a water environment at the same time. Their molar fraction is governed both internally by their chemical structure[82] and externally by the pH of an environment.

If radicals are neutralized by mechanisms inaccessible to other forms, a seemingly small amount of one of them may be critical in accurately measuring scavenging activity. At the given pH, for example, it is possible that the antioxidants have already deprotonated all of the hydroxyl groups and thus exhibit only electron-related channels,[36,85,102,126] whereas the studied radical is efficiently neutralized solely by formal hydrogen atom transfer. Similarly, with each subsequent dissociation, species are less likely to remove another proton, making routes that include its donation, e.g. sequential proton-loss electron transfer or sequential electron transfer-proton transfer, more energetically demanding; on the other hand, electron-donating processes are expected to occur more easily for them.

There are several methods that can be used to estimate dissociation constants and deprotonation pathways. The oldest ones, such as *direct*, *proton exchange*, *hybrid cluster continuum*, and *implicit–explicit*, rely on thermodynamic cycles and have previously been exhaustively discussed in the literature[176,177] and are thus just briefly mentioned here.

In the *direct* approach, an antioxidant may either (a) adhere to the Arrhenius theory and dissociate directly into anion and proton (Scheme 1a), (b) obey Brønsted–Lowry acid–base theory and react with a water molecule to form conjugated pairs of acid and base (Scheme 1b), or (c) react in the same way as the previous one but in a more sophisticated version in which the formed ion is also solvated by an arbitrary number of water molecules (Scheme 1c).

Regardless of the picked cycle, ΔG_s^* represents the free energy of deprotonation, which is calculated using eq 6

$$\Delta G_s^* = \Delta G_{gas}^\circ + \sum_{i=1}^{\text{N products}} n_i \Delta G_{solv}^*(i) - \sum_{j=1}^{\text{N reactants}} n_j \Delta G_{solv}^*(j) \quad (6)$$

Then, pK_a is determined using a mathematical formula (eq 7)

$$pK_a(\text{AntoxOH}) = \frac{\Delta G_{s(\text{AntoxOH})}^*}{2.303RT} \quad (7)$$

Despite the fact that one of the major drawbacks for this method is it requires proton or hydronium ion enthalpies, for which theoretical studies do not perfectly match, due to the impact of different solvation models used[178] or methodology,[179] it is still widely used[27,114,139] owing to its simplicity. The question and recommended values of solvation enthalpies have been extensively elaborated by Marković and coworkers.[178,180,181]

Another way for determining pH is the *relative method* or *isodesmic method*. It is based on the proton exchange equilibrium between the acid of interest and the conjugated base of the reference acid and is represented by the following general chemical reaction

$$\text{AntoxOH} + \text{Ref}^- = \text{AntoxO}^- + \text{HRef}$$

The acid–base pair of a reference chemical is defined as HRef/Ref$^-$, and pK_a is computed in the same way as in the direct method but with a modified form of the previously supplied equation, given here as eq 8

https://doi.org/10.1021/acs.jcim.2c00104
J. Chem. Inf. Model. 2022, 62, 2639–2658

$$pK_a(\text{AntoxOH}) = \frac{\Delta G^*_{s(\text{AntoxOH})}}{RT\ln(10)} + pK_a(\text{HRef}) \quad (8)$$

Although this method has been shown to produce accurate results,[58,69] it requires HRef to be as structurally close to the HA as possible, and also the knowledge of the experimental value for pK_a(HRef).

Among the newer approaches, the *parameters fitting method*[182,183] stands out not only due to its much simpler computation protocol but also the accuracy reported in the number of studies that have used it.[36,41,46,73,85,101,112,126] It employs a linear regression model to determine pK_a values for hydroxyl, carboxylic, amino, and thiol groups in a water solvent. Mathematically, it is expressed by eq 9

$$pK_a(\text{AntoxOH}) = m\Delta G^*_{\text{AntoxOH/AntoxO}^-} + C \quad (9)$$

where $\Delta G^*_{\text{AntoxOH/Antox}^-}$ denotes the difference in Gibbs free energy between the antioxidant's conjugated base and the corresponding acid, and m and C are empirical parameters available for 20 different functionals, each in one of four Pople's basis sets.

The former, however, is restricted solely to the water solvent. The solution is the *empirical conversion method*[184] presented recently. Although it does not allow for the calculation of pK_a values from scratch, the authors claim that it is useful for converting empirically determined dissociation constants in one solvent to any other with a little error.

Because both, the *parameters fitting method* and the *empirical conversion method*, were developed on strong experimental foundations, combining them in critical situations may not be such a bad idea. However, further testing is required to confirm this.

ELECTRONIC STRUCTURE INVESTIGATIONS

Intrinsic Reactivity Indices. A comprehensive study that covers the entire spectrum of antioxidative activity is difficult and time-consuming process. The intrinsic reactivity indices (Table 1) can be evaluated to obtain preliminary data that will guide further steps of the research. Although they do not consider the radical scavenged, the evaluation of preferred reaction paths of isolated species, identification of the most promising ones for a specific goal, and comparisons across antioxidants with similar chemical nature and modes of action is given by them.

Notably, reactivity indices can be calculated vertically or adiabatically, that means with or without orbital relaxation. IP and EA are particularly important in Marcus theory for calculating the activation energy of electron transfer mechanisms and are thus mostly established in this context. The following equations (eq 10 and eq 11) are used to determine their vertical values

$$E_{(N-1)}(g_N) - E_N(g_N) = \text{vertical IP} \quad (10)$$

$$E_{(N)}(g_N) - E_{N+1}(g_N) = \text{vertical EA} \quad (11)$$

The adiabatic ones, on the other hand, are calculated as (eq 12 and eq 13)

$$E_{(N-1)}(g_{N-1}) - E_N(g_N) = \text{adiabatic IP} \quad (12)$$

$$E_{(N)}(g_N) - E_{N+1}(g_{N+1}) = \text{adiabatic EA} \quad (13)$$

Table 1. Names, Associated Reactions, and Explanations of Intrinsic Reactivity Indices

Name (typical acronym)	Related reaction	Brief description
Ionization potential (IP)	$\text{Antox(OH)}_n \rightarrow \text{Antox(OH)}_n^+ + e^-$	The ability to contribute an electron, which is interpreted as a willingness to oxidize itself. The lower the IP, the greater the likehood of antioxidant protection through electron transfer via electron donation. This is sometimes referred to as ionization energy (IE) in the literature.
Electron affinity (EA)	$\text{Antox(OH)}_n + e^- \rightarrow \text{Antox(OH)}_n^-$	The ability to accept an electron, which can be interpreted as a desire to reduce itself. The lower the EA, the more likely antioxidant protection through electron transfer via electron acceptance.
Bond dissociation enthalpy (BDE)	$\text{Antox(OH)}_n \rightarrow \text{Antox(OH)}_{n-1}\text{O}^\bullet + H^\bullet$	The amount of energy required to break the O−H bond during homolytic fission, which can be interpreted in the context of the radical's stability. The lower the BDE values, the more active the corresponding −OH residue is in the hydrogen atom transfer mechanism and the more stable the radical formed.
Proton affinity (PA)/Proton dissociation enthalpy (PDE)	$\text{Antox(OH)}_n \rightarrow \text{Antox(OH)}_{n-1}\text{O}^- + H^+$	The amount of energy required to break the bond during heterolytic fission, which can be interpreted as the anion's stability. The lower the PA/PDE value, the more the corresponding −OH residue will be deprotonated. PA is defined as the inverse of the enthalpy change in a gas phase reaction between an electrically neutral chemical species and a proton to form the conjugated acid of the latter, whereas PDE is the deprotonation of a radical cation in any medium.

https://doi.org/10.1021/acs.jcim.2c00104
J. Chem. Inf. Model. 2022, 62, 2639−2658

Table 2. Names, Mathematical Formulations, and Descriptions of Indices Related to Frontier Molecular Orbitals Theory

Name (typical acronym)	Related formula	Brief description
HOMO−LUMO gap (HLG)	$\mathrm{HLG} = \mathrm{IP} - \mathrm{EA}$	Represents the ease with which the electron in a molecule can be excited from HOMO to LUMO. The lower it is, the easier the electron migrates from one another, and the radical reaction proceeds more quickly because it is more kinetically stable.
Electronegativity (χ)	$\chi = \frac{\mathrm{IP} + \mathrm{EA}}{2} = -\mu$	The general proclivity to attract electrons.
Chemical potential (μ)	$\mu = -\frac{\mathrm{IP} + \mathrm{EA}}{2} = -\chi$	Indicates the direction of charge flow as well as the capacity to contribute or accept it. Electrons will migrate from high to low μ locations in a quantity proportional to changes in μ, with a corresponding stabilizing energy μ.[2]
Global hardness (η)	$\eta = \frac{\mathrm{IP} - \mathrm{EA}}{2}$	Measures the resistance to electron cloud polarization caused by a minor chemical disturbance or a change in electron number.
Global softness (S)	$S = \frac{\eta}{2}$	The ability to accept electrons. It is inversely proportional to chemical hardness.
Electrophilicity (ω)	$\omega = \frac{\mu^2}{2\eta}$	The ability of a system to acquire a partial charge. When two molecules are involved in a chemical reaction, the one with the higher value is considered the acceptor, while the one with the lower value is considered the donator. It is advised to be used to demonstrate the efficacy of electron donation in compounds with extremely low IP values.

Table 3. Names, Mathematical Formulations, and Descriptions of DAM-Related Indices

Name (typical acronym)	Related formula	Brief description
Electrodonating power ($\omega-$)	$\omega^- = \frac{(3\mathrm{IP} + \mathrm{EA})^2}{16(\mathrm{IP} - \mathrm{EA})}$	The ability of a chemical system to provide a fractional amount of charge. The lower the $\omega-$, the more likely it is that the molecule will behave as an electron donor in weak interactions with other species.
Electron-accepting power ($\omega+$)	$\omega^+ = \frac{(\mathrm{IP} + 3\mathrm{EA})^2}{16(\mathrm{IP} - \mathrm{EA})}$	The ability of a chemical system to receive a fractional amount of charge. The greater the $\omega+$, the more likely it is that the molecule will behave as an electron acceptor in weak interactions with other species.
Donor index (R_d)	$R_d = \frac{\omega^-_{\mathrm{AntoxOH}}}{\omega^-_{\mathrm{Na}}}$	
Acceptor index (R_a)	$R_a = \frac{\omega^+_{\mathrm{AntoxOH}}}{\omega^+_{\mathrm{F}}}$	
Relative value of electron acceptance (REA)	$\mathrm{REA} = \frac{\mathrm{EA}_{\mathrm{AntoxOH}}}{\mathrm{EA}_{\mathrm{F}}}$	
Relative value of electron donation (RIE)	$\mathrm{RIE} = \frac{\mathrm{IP}_{\mathrm{AntoxOH}}}{\mathrm{IP}_{\mathrm{Na}}}$	

where E_N, $E_{(N-1)}$, and E_{N+1} denote the total energies of the N, $N-1$, and $N+1$ electron systems, respectively, computed at ground state geometries of (g_N), (g_{N-1}) and (g_{N+1}) systems.

The Hammet sigma constant is one of the tools that draws from reactivity indices. It reflects the electron withdrawing or donating capacities of substituents connected to the aromatic moiety and thus can be applied to assess their impact on the intrinsic reactivity indices in a semiquantitative manner.[22,23,32,127] They can be also used as a features of quantitative structure−activity relationship (QSAR) models, which numerically relate them and other descriptors to experimental data.[11,24,43] Recently, an extensive paper on QSAR development and validation was published.[185]

Frontier Molecular Orbitals. The energy and distribution of frontier molecular orbitals, specifically the highest-occupied molecular orbital (HOMO), a nucleophilic part of the molecule, and the lowest-unoccupied molecular orbital (LUMO), an electrophilic part of the molecule, can be directly linked to antioxidative activity.[186] This is because Janak's theorem[187,188] states that the energies (ε) of HOMO and LUMO are related to ionization potential (eq 14) and electron affinity (eq 15), respectively, via the following relationship:

$$-\varepsilon(\mathrm{HOMO}) = v\mathrm{IP} \tag{14}$$

$$-\varepsilon(\mathrm{LUMO}) = v\mathrm{EA} \tag{15}$$

A molecule with a low HOMO eigenvalue is likely to be a poor electron donor, whereas a molecule with a low LUMO eigenvalue is likely to be a good electron acceptor. Analyzing their values allows for the initial elucidation of the antiradical activity. Although the majority of naturally ocuring radicals are electrophillic, and so the interaction between their SOMO and antioxidants' HOMO is of the greatest importance, there also exist nucleophilic ones, typically carbon-centered, which scavenging potential is subjected to the overlap between SOMO of the reactive specie and LUMO of the scavenger. In addition, visualizing HOMO allows for a prediction of which molecular site is more vulnerable to radical attack[28,50,116], but presented later Fukui functions are more reliable option.

These approximations of orbitals egeinvalues as ionization potential or electron affinity, however, ignore electron correlation and are highly dependent on the method and basis set employed[27,52,123,153]. This poses further problems for they serve as the foundation for a slew of global descriptive parameters related to the electrophilic character of the species (Table 2)[189] meaning their improper values may lead to further errors in the study and invalid conclusions. Given the importance of being as precise as possible, direct computations, are strongly advised. On the other hand, M062X/6-311G(d,p) level of theory has been found to approximate energies of frontier molecular orbitals with an error no greater than 0.5eV from the ones calculated in the direct vertical manner.[153]

https://doi.org/10.1021/acs.jcim.2c00104
J. Chem. Inf. Model. 2022, 62, 2639−2658

To ensure the quality of vertical energies obtained, an electron propagator theory (EPT)[190,191] and a partial third-order quasiparticle theory (P3)[191] can be exploited. These theories lay the groundwork for the systematic inclusion of electron correlation in a one-electron model of molecular electronic structure. They have been shown to produce lower mean errors than any other open shell techniques when compared to experimental trial results[192] and are now wiedly used.[46,101,112] For the EPT estimations to be valid, the pole strength (PS) values must be greater than 0.80−0.85.[193,194]

Electron and Hydrogen Donation Properties. To do quick and simultaneous comparisons of the relative electron-donating and electron-accepting properties of a set of species the donator-acceptor map (DAM) is a right choice.[195] It is based on the assumption that in a simple charge−transfer model the response of a molecule submerged in an idealized environment that can either remove or donate charge can be represented by a quadratic interpolation for the energy as a function of the number of electrons.[196,197] Therefore, DAM exhibits the antioxidant's tendency in charge-related processes in terms of electron-donating (ω^-) and electron-accepting (ω^+) powers (Table 3).

The substance is classified into one of four distinct zones (Figure 2) based on precalculated donor (R_d) and acceptor (R_a)

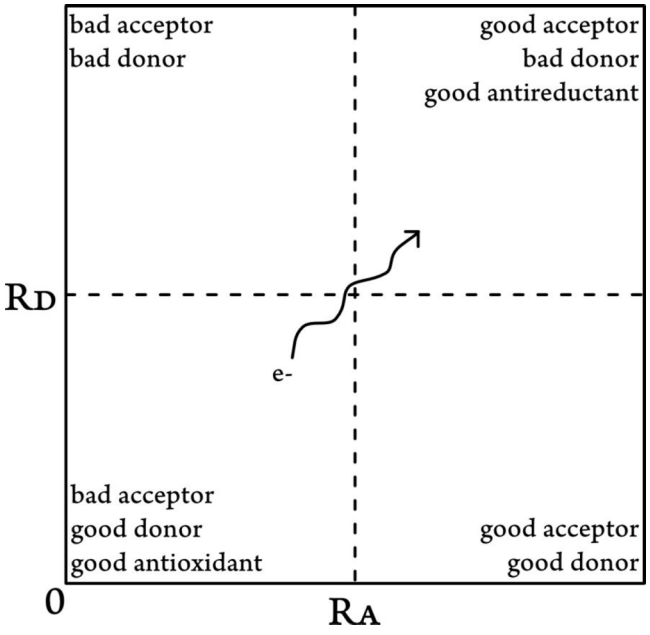

Figure 2. Schematic representation of donator−acceptor map.

indices: (1) the excellent antiradical zone (lower right), where it is both a superior electron donor (small R_d) and acceptor (high R_a), (2) the worst antiradical zone (upper left), where it is both a poor electron donor (high R_d) and a poor electron acceptor (small R_a), (3) the good antireductant zone (upper right), where it is a fine electron acceptor (high R_d and R_a) and thus an effective antiradical, and (4) the strong antioxidant area (lower left), where its good electron donor properties manifest (small R_d and R_a).

R_d and R_a are valued for their electron-donating and electron-accepting powers, respectively, and are defined in relation to the electron-accepting power of fluorine ($\omega_F^+ = 3.40$) and electron-donating power of sodium ($\omega_{Na}^- = 3.46$). F^- and Na^+ are used as references due to their high electron-accepting and electron-donating capacities. ω_F^+ and ω_{Na}^- can be calculated using experimental data.[32] If $R_a < 1$, the substance is a poorer electron acceptor than F, and if $R_d > 1$, it is a poorer electron donor than Na.

Three of the four zones represent the intended antioxidative activity. In the above graph, the electron flow goes from species in the bottom left to species in the top right. When comparing substances, DAM helps to predict which will behave as stronger or weaker oxidizers or reducers,[85] while also accounting for the effects of the environement.[62,71] It is good to remember, there is a general trend of increasing electron-donating properties with each subsequent dissociation, so polyanionic species shall generally have lower R_d values than neutral of cationic forms.[50,91]

Full electron−donor−acceptor map (FEDAM), an improved version of DAM, has been developed to account for the nature of the interacting free radical, which can have such a significant impact that it can even invert the relative importance of the free radical scavenging mechanisms.[198] FEDAM is based on the relative values of electron acceptance (REA) and electron donation (RIE) indices derived from vertical IP and vertical EA, again with Na and F atoms used as references. These are plotted on a map in the same way that DAM is but for both antioxidants and radicals. It has been used to evaluate antioxidant activity of melatonin, as well as its metabolites and derivatives.[101,105]

The electron- and hydrogen-donating ability map for antioxidants (eH-DAMA)[101] is another approach to enhance DAM. It was designed to identify compounds that are good donors in both electron transfer (low ω) and hydrogen atom transfer (low BDE). It is similar to DAM, but the axes changes, so the Y axis corresponds to ω, while the X axis refers to BDE. As a result, the species in the left-bottom region are more likely to work in both directions, making them particularly valuable as radical scavengers, such as new sesamol[112] or melatonin derivatives[101], or modified p-coumaric acid analogs with neuroprotective activity.[46] In most cases, parent molecules, oxidants, or reference antioxidants, e.g. Trolox, are included for comparison purposes.[46,112]

Radical Attack Site. Frontier molecular orbital theory introduces a numerical method for investigating the reactivity of individual sites of molecule in three types of reactions. Fukui functions[199] were proposed to represent the difference in electron density at a given point, $\rho(r)$, as a function of the number of electrons, N, at a given external potential, $v(r)$ (eq 16). This is based on the notion that the optimal path for a reagent to approach the other species is the one with the highest initial fluctuation of the electronic chemical potential, μ.

$$f(r) = \left[\frac{\delta\mu}{\delta v(r)}\right]_N = \left[\frac{\partial\rho(r)}{\partial N}\right]_{v(r)} \tag{16}$$

Integrating over that equation for individual atoms in a molecule yields condensed Fukui functions (eqs 17−19), which are a more convenient way of predicting the reaction site than visualization of HOMO or LUMO orbitals. In general, the higher the value, the more reactive this position is to the specific type of attack. For an arbitrary atom A, these functions are defined as

$$f_A^- = q_{N-1}^A - q_N^A, \quad \text{for electrophilic attack} \tag{17}$$

$$f_A^+ = q_N^A - q_{N+1}^A, \quad \text{for nucleophilic attack} \tag{18}$$

https://doi.org/10.1021/acs.jcim.2c00104
J. Chem. Inf. Model. 2022, 62, 2639−2658

$$f_A^0 = \frac{[f_A^+ + f_A^-]}{2} = \frac{[q_{N-1}^A + q_{N+1}^A]}{2}, \text{ for radical attack} \quad (19)$$

where q_{N-1}^A, q_{N+1}^A represent charges of $(N-1)$ and $(N+1)$ systems obtained vertically from the optimized ground state geometry (N) with charge q_N^A. This ensures that the values are solely determined by the atom's electronegativity and electron density location. At the same time, because of that the atomic charge values used to estimate condensed Fukui functions are heavily reliant on population analysis method.[124,200,201] Given their varied formulations,[202] the condensed Fukui functions may exhibit significant mutual discrepancies—even negative values[28]—but this has already been explained as a result of the small interatomic distances between atoms.[203,204] So Atoms-in-Molecule tend to overestimate them;[204] Natural Population Analysis is heavily influenced by the functional, and basis set chosen;[205] and ESP derived charges, such as ChelpG, have nonsmooth geometry dependence.[200] Also a solvent may also affect the final result.[124] Some studies propose stockholder charge partitioning approaches in this purpose, particularly Hirschfeld analysis,[15,64,123] since it yields values for which condensed Fukui functions correlate well with the expected data. In fact, a "dual descriptor" better illustrates susceptibility for electrophilic−nucleophilic attack,[206] but these types of reactions are beyond the scope of antiradical activity studies.

Redox Potentials. As it was already mentioned, primary activity of antioxidants is related to the direct reduction of radicals. Therefore, the viability of this process can be assessed in terms of electrochemical potentials.[207] The Born−Haber thermodynamic cycle is one universal method due to the common pattern of reactivity, and a half-reaction describing that process is always denoted by

$$\text{AntoxOH}_{(aq)}^{+\bullet} + e^- \rightarrow \text{AntoxOH}_{(aq)}$$

for which the standard reduction potential can be calculated using the Nernst equation (eq 20)

$$E_{red(aq)}^{\circ} = -\frac{\Delta G_{red}^*}{nF} \quad (20)$$

where ΔG_{red}^* denotes the standard Gibbs free energy of the reduction, and n is the number of electrons transferred and F the Faraday's constant (23.06 kcal/molV). According to the Born−Haber cycle, ΔG_{red}^* equals

$$\Delta G_{red}^* = G^*(\text{AntoxOH}^{+\bullet}) - G^*(\text{AntoxOH}) - nG^{\circ}(e^-) \quad (21)$$

with $G^{\circ}(e^-)$ being free energy of one electron in the gas phase (−0.876 kcal/mol at 298 K). When comparing results to those obtained experimentally, the computed values must be reduced by an absolute potential of the reference electrode, for example, a standard iron electrode or a standard hydrogen electrode.

Notably, because certain compounds may be partially deprotonated at a given pH, and anions have a lower capacity to donate electrons than neutral forms, they also influence the overall reduction potential. As a result, the average can be calculated accordingly to eq 22

$$E = E^{\text{AntoxOH}^{+\bullet}|\text{AntoxOH}} + \frac{RT}{F}\ln(f_{\text{AntoxOH}^{+\bullet}}) - \frac{RT}{F}\ln(f_{\text{AntoxOH}}) \quad (22)$$

where $E^{\text{AntoxOH}+\bullet|\text{AntoxOH}}$ represents the initial reduction potential, and $f_{\text{AntoxOH}^{+\bullet}}$ denotes the population of the oxidized species that are reduced to produce the species with population $f_{\text{AntoxOH}\cdot}$.

Topology Analysis. Hydrogen bonds and weak interactions are important in stabilizing radicals or transition states rendering reactions to be more feasible, for example, by lowering BDE values.[50] Bader's Quantum Theory of Atoms in Molecules (QTAIM) can be used to quantify their strength[208,209] and thus has been widely applied in antioxidants research.[31,58,62,103,122,130] Despite the analysis's complexicity, specialized tools such as the Multiwfn software[210] eases it.

The nature of chemical bonds at bond critical points (BCPs) can be mathematically described by electron densities, ρ, and their associated Laplacian, $\nabla^2\rho$. The theoretical background is explained in detail in Bader's paper;[208] here, it will only be mentioned that BCPs of primary importance in such studies correspond to (3,−1) critical points, being the saddle points with a maximum of electron density in two directions of space and a minimum in the third, and that the number of BCPs must obey the Poincare−Hopf rule.[211]

The presence of a bond path between two atoms with a BCP in the middle is the first sign of a bond presence.[208,215] A second criterion for defining it is that the values of ρ(BCP) and $\nabla^2\rho$(BCP) are positive, in ranges of 0.002−0.035 and 0.024−0.139, respectively.[215−217] $\nabla^2\rho$(BCP) can be expanded as the sum of the eigenvalues λ_1, λ_2, λ_3, obtained by diagonalizing the Hessian of the electron density and mutually related as $\lambda_1 < \lambda_2 < \lambda_3$. They can be used to calculate the ellipticity parameter, $\varepsilon = \frac{\lambda_1}{\lambda_2} - 1$, which quantifies the amount of charge that accumulates preferentially. A large ε indicates topological instability and, as a result, an easily ruptured bond. The λ_3 specifies how easily the BCP can be moved along the bond path,[208] and the higher the value is, the stronger the interaction is. A local formulation of the virial theorem[208] relates $\nabla^2\rho(BCP)$ to electronic topological parameters by eq 23

$$\frac{\nabla^2\rho(\text{BCP})}{4} = 2G(\text{BCP}) + V(\text{BCP}) \quad (23)$$

where G(BCP) is the Lagrangian kinetic electron density, and V(BCP) represents the potential electron density (also known as the virial field).

Positive $\nabla^2\rho$(BCP) values indicate that G(BCP) is greater than V(BCP), implying that charge is being depleted along the bond path, as is typical of closed-shell interactions such as hydrogen bonding, ionic bonds, and van der Waals. Its negative values, on the other hand, indicate an excess potential energy at BCP in the form of internuclear charge concentration, which corresponds to covalent interactions; in this case, an electron density is localized in between two nuclei and is mutually accessible to both of them.[212]

Similarly, the $-G(\text{BCP})/V(\text{BCP})$ ratio can be used for that purpose, because $-G(\text{BCP})/V(\text{BCP}) > 1$ indicates that the intramolecular bond is closed and noncovalent, while $0.5 < -G(\text{BCP})/V(\text{BCP}) < 1$ points out that it is shared—for example partially covalent or ionic.[208,213,214]

Espinosa and coworkers[219,220] demonstrated that interatomic interaction energy can be related to potential electron energy density at BCP using the following expression

$$E_{HB} = \frac{V(\text{BCP})}{2} \quad (24)$$

https://doi.org/10.1021/acs.jcim.2c00104
J. Chem. Inf. Model. 2022, 62, 2639−2658

The above relationship, according to Rozas et al.,[218] allow hydrogen bonds to be classified as weak (E_{HB} < 12.0 kcal/mol), when $\nabla^2\rho$(BCP) > 0 and H(BCP) > 0, medium (12.0 < E_{HB} < 24.0 kcal/mol) if $\nabla^2\rho$(BCP) > 0 and H(BCP) < 0, or strong (E_{HB} < 24.0 kcal/mol) when $\nabla^2\rho$(BCP) < 0 and H(BCP) > 0, where H(BCP) denotes the density of electrons total energy, G(BCP) + V(BCP).

This is one of the most useful methods for calculating the energy of hydrogen bond interactions. Furthermore, Korth et al.[221] demonstrated how to compute the relative intramolecular hydrogen bond enthalpy by comparing the sum of the conformer's electronic and thermal enthalpies with intramolecular hydrogen bonds.

However, QTAIM analysis must to be used with caution in course of the studies. The molecule's wavefunction, which is used to evaluated the aforementioned interactions, is determined by the functional and basis set used. As evidenced from refs 222 and 223, no relevant relationship between climbing Perdew's Jacob's ladder rungs and BCP densities was reported. The basis set, on the other hand, appears to be of primary concern. It has been demonstrated[224] that small, double-ζ basis sets from Pople or Dunning's families are insufficient to accurately assess the properties of BCP related to multiple and polar bonds, as well as weak hydrogen bond interactions. Instead, at least triple-ζ are recommended, which is plausible in the context of the current trend in their choice in the studies on antioxidants.

Natural Bond Orbitals. One of the primary requirements for an antioxidant to effectively scavenge free radicals is that it becomes stable after the reaction. The spin density distribution throughout the molecule, which is often larger for conjugated systems, can be used to examine that property;[28,33,50,82] however, natural bond orbital analysis[225−228] represents a much more detailed investigation into the topic.

Refining the wavefunction into a Lewis-like structure corresponding to lone pairs and bonds gives an opportunity to track charge transfer by examining changes in the electron density at bonds, investigate hybridization of the orbitals and bonding interactions, as well as study delocalization and hyperconjugation effects.[10,34,61,67,85,103,123] During the natural bond orbital analysis, the stabilization energy, $E^{(2)}$, is derived for the electron transfer from filled donor orbital, i, to an empty acceptor orbital, j, and is related by eq 25

$$E^2 = -q^i \frac{(F_{ij})^2}{(E_j - E_i)} \tag{25}$$

where F_{ij} is the off-diagonal Fock matrix element and q^i the orbital occupancy, and E_j and E_i are diagonal elements. The intrepretion is clear —, the greater the E^2 energy, the greater degree of interaction.

NBO analysis, just like QTAIM, also requires careful application. Alhough it is a straightforward and advantageous method, at the same it is heavily reliant on the geometry of the compound, which stems from the partitioning scheme of the electron density matrix and the localized nature of molecular orbitals. A simple, yet excellent, example of this can be found in the paper of Benassi and Fan[229] where the authors reported on how the delocalization energy and orbital occupancy number differ in pyridine across its seven normal modes and small changes along the displacement coordinates. It has been demonstrated that even minor shift can result in significantly different $E^{(2)}$ values, which is expected to be amplified in the case of larger antioxidant structures.

REACTIVITY

Thermochemistry. In reality, the antioxidant's ability to scavenge radicals is influenced not only by the antioxidant itself but also by the species with which it interacts. As a result, thermochemical calculations of known pathways (Table 4) produce far more useful data than intrinsic reactivity indices alone; one way to illustrate them is with O'Ferrall−Jencks diagrams[83,86] (Figure 3). However, before proceeding, a foreword is required: hydroxyl radical, $^{\bullet}$OH, is so reactive that it quickly reacts with almost any molecule in its vicinity at diffusion-limited rates, before an antioxidant can actually reach it. For this reason, it is skipped from computations and radicals with intermediate to low reactivity are chosen instead for assessing the antiradical potential.[230−232] Peroxyl radicals, ROO$^{\bullet}$ (such as $CH_3OO^{\bullet}$ or $OOH^{\bullet}$),[233,234] are one of these because their half-lives are long enough that they can be intercepted before oxidizing biological targets.[235,236] Although acid-base equilibrium of hydroperoxide equals 4.8, what means that $O_2^{\bullet-}$ is typically present in physiological conditions, it is not very reactive species and the oxidation damage are primiarly steming from its protonated form.[237] $CCl_3OO^{\bullet}$ can also be considered because it is used in experiments to simulate larger radicals.[238] Another possible reduction target might be the H_2O_2/O_2 pair, which is more difficult to neutralize than other reactive oxygen species.[239]

The polarity of the environment also has an effect on reaction energetics. To begin with, it should come as no surprise that reactions generating neutral species, such as RAF or HAT, perform better in nonpolar solvents than reactions that produces ions. This is due to the fact that nonpolar media do not provide enough solvation to stabilize charged species through the charge separation, thereby propelling the reaction forward. In consequence, such reactions are unlikely to occur in a significant number, and conventional studies in nonpolar media focus solely on RAF and HAT, with the remaining pathways being completely ignored.[60,63,106,121,139,143]

Furthermore, the first step in a multistep mechanism is thermodynamically significant and so determining its energetics allows for assessing reaction's feasability, simplifying the analysis by rejecting unfavorable pathways. Because BDE, IP, and PA are the primary indices of the HAT, SET-PT, and SPLET,[240−243] they can be used for this purpose.

Moreover, because SPLET mechanism is initiated by proton dissociation, which proclivity is controlled by the environment's pH and acid−base equilibrium, the SET and SPLET processes are extremely closely coupled due to the spontanous. If molar fractions are being considered at the outset, the second step of SPLET actually controls an antioxidant's reactivity, and in this case the entire mechanism becomes equivalent to SET; namely, it is identical to the SET reaction for an acid−base species with $N - 1$ protons. Herein, I will just mention that it is also an electrostatic potential map, which is a useful tool for distinguishing between electrophilic and nucleophilic centers, highlights positively charges hydroxyl hydrogen to be likely involved in proton dissociation mechanisms.[28,68]

Finally, because IP and EA values govern electron flow between antioxidant and radical, they can be used to estimate the direction of the SET mechanism, providing an early picture of the process. In general, the bare minimum for SET reactions with electrophilic radicals is IP(antioxidant) < EA(radical) and

https://doi.org/10.1021/acs.jcim.2c00104
J. Chem. Inf. Model. 2022, 62, 2639−2658

Table 4. Naming, Associated Reactions, and Descriptions of the Most Commonly Studied Antioxidative Reaction Pathways

Name (typical acronym)	Related reaction	Description
Radical adduct formation (RAF)	$Antox(OH)_n + X^\bullet \rightarrow [Antox(OH)_nX]^\bullet$	In a single step, the radical forms an adduct with the antioxidant, spreading the spin density across the newly formed molecule. The preferred reaction site is determined by the degree of the unpaired electron delocalization.
Hydrogen atom transfer (HAT)/Proton coupled electron transfer (PCET)	$Antox(OH)_n + X^\bullet \rightarrow Antox(OH)_{n-1}O^\bullet + HX$	A one-step mechanism in which an O−H bond is homiletically broken and a hydrogen atom is transferred from antioxidant to free radical, resulting in a more stable antioxidant radical. Low BDE values are common in compounds that promote this path. In the electrochemical sense, it is a reduction process. Although the products of HAT and PCET reactions are identical, the former involves the coordinated transfer of a proton and an electron as a single entity, whereas PCET involves the process of two separated particles, not necessarily from the same sets of orbitals. Formal HAT refers to chemical reactions that have not been defined as HAT or PCET.
Single electron transfer (SET)	$Antox(OH)_n + X^\bullet \rightarrow Antox(OH)_n^{\bullet+/\bullet-} + X^{-/+}$	Depending on the mutual IP and EA values, a single electron transfer occurs from an antioxidant to a radical or from a radical to an antioxidant. The deprotonation influences the thermochemical viability of the SET process to some extent.
Sequential electron transfer-proton transfer (SET-PT)		It occurs in two steps: first, a radical cation $Antox(OH)_n^{\bullet+}$ is formed by electron transfer from an antioxidant to a free radical, and then, it deprotonates to form $Antox(OH)_{n-1}O^\bullet$ species. The first step is described by the IP values, while the second step is described by the PDE values.
1. Electron transfer	1. $Antox(OH)_n + X^\bullet \rightarrow Antox(OH)_n^{\bullet+} + X^-$	
2. Proton transfer	2. $Antox(OH)_n^{\bullet+} \rightarrow Antox(OH)_{n-1}O^\bullet + H^+$	
Sequential proton loss-electron transfer (SPLET)		The mechanism is divided into two steps: first, an antioxidant is deprotonated (as described by PA), and then, an electron transfer occurs from the deprotonated antioxidant to a free radical (described by IP). Because pK_a values influence the amount of deprotonated species in aqueous solution, knowing their number *a priori* can assist in determining the relative importance of this process.
1. Proton loss	1. $Antox(OH)_n \rightarrow Antox(OH)_{n-1}O^- + H^+$	
2. Electron transfer	2. $Antox(OH)_{n-1}O^- + X^\bullet \rightarrow Antox(OH)_{n+1}O^\bullet + X^-$	
Sequential proton loss−hydrogen atom transfer (SPLHAT)		The mechanism is identical to SPLET, except that instead of an electron, a hydrogen atom is transferred in the second step. As a result, antioxidants containing at least two hydroxyl groups are particularly appealing. PA describes the first step, and BDE describes the second.
1. Proton loss	1. $Antox(OH)_n \rightarrow Antox(OH)_{n-1}O^- + H^+$	
2. Hydrogen atom transfer	2. $Antox(OH)_{n-1}O^- + X^\bullet \rightarrow Antox(OH)_{n-2}(O)_2^\bullet + HX$	

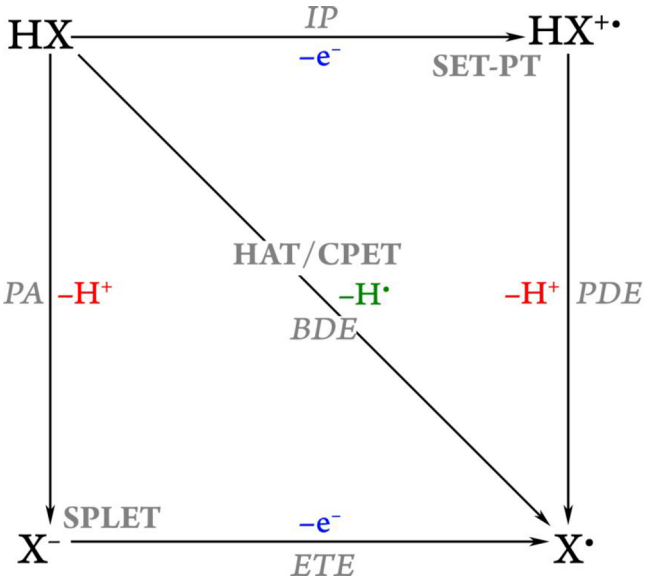

Figure 3. O'Farell−Jencks diagram of each single step involved in common reaction mechanisms.

opposite holds true for the nucleophilic ones. In case of not so easily recognizable species, a general rule of knowing that electrons flow from the structure of lower IP to the structure of greater EA, makes it possible to predict which molecule will undergo oxidation and which will undergo reduction, and the reverse path can be thereby ignored.

One final point to mention about thermochemical calculations is that they require the Gibbs free energies of electron, proton, and hydrogen. The very last can be estimated directly at the applied level of theory, but the proton and electron cannot, at least not in a straightforward manner, necessitating the use of widely varying reference values.[178,180,181,244]

Kinetics. An antioxidant is any substance that, even at low concentrations, significantly delays or prevents the oxidation of radical target. Therefore, it must not only react spontaneously with the oxidizing agent, but it must also react faster than the target it is designed to protect.[245,246] This aspect can only be modeled using kinetic studies, which account for facets skipped by thermochemical studies—tunneling effects, weighted contribution of different mechanisms and different species to total antioxidative potential, or adherence to the Bell−Evans−Polanyi principle[3]—and is thus critical for accurately assessing antioxidative behavior.

Although spontaneity is an important criterion for chemical reactivity, it is not always enough because an exergonic reaction can occur at either fast or slow rates. When drawing conclusions from thermochemical data without considering kinetics, the Bell−Evans−Polanyi[247,248] principle, which states that the most exergonic processes have the lowest activation energies and are thus kinetically favored, is implicitly assumed to be followed.[3] On the other hand, ignoring a reaction path due to difficulties in locating a transition state may result in a more significant error than accepting the given rule wihout its confirmation, especially if it was discovered to hold true for a structurally similar compounds.[118] It has been recently evidenced that Gibbs free energy is actually proportional to the activation energy of hydrogen atom transfer, and hence reaction rate of this mechanism.[90,249,250]

Endergonic channels do not need to be included in kinetic calculations in general because even if they occur at high rates,

https://doi.org/10.1021/acs.jcim.2c00104
J. Chem. Inf. Model. 2022, 62, 2639−2658

they are reversible to the point where no products are detected. However, moderately endergonic processes (typically with ΔG° < 10.0 kcal/mol) may still contribute to antioxidant capacity and should be addressed, particularly if their products evolve into other species quickly, providing a driving force, or the reaction barriers are low.[182] This is the case for some RAF reactions,[82] but it is particularly common for SET, where thermochemical and kinetic data may show opposing trends; in some cases, the mechanism may be associated with positive Gibbs energies and still be relevant, as has been demonstrated in a number of previously reported studies.[36,46,73,82,154] Highly exergonic SET reactions involving donors with very low IP (such as monoanionic or polyanionic species) may, on the other hand, be found in the inverted region of the Marcus parabola, where that reaction barriers increase as ΔG° decreases what is often to be found for Gibbs free energies much lower than negative of reorganization energy.[251−253] Despite this is an unexpected behavior, it underlines that particles with extremely low IP are unlikely to be efficient free radical scavengers.[46,101,125] That is why using ionization potentials may be misleading, and electron-donating power or electrophilicity is far superior because, while it also relies on IP, it does so in a nonlinear fashion, with the shape of this dependency resembling the Marcus parabola.[46,101,112]

The activation barrier of a reaction is determined by the energy difference between the transition state and the reactants. However, in the case of electron-related processes, assessing it is not so straightforward. The barrier of electron transfer reaction ($\Delta G^{\neq}_{ET}$) is calculated in a different way, using the Marcus theory[253−255] (eq 26), which defines it in terms of the reaction adiabatic free energy (ΔG^0_{ET}) and nuclear reorganization energy (λ)

$$\Delta G^{\neq}_{ET} = \frac{\lambda}{4}\left(1 + \frac{\Delta G^0_{ET}}{\lambda}\right)^2 \tag{26}$$

The reorganization energy is calculated as the difference between the vertical (ΔE_{ET}) and adiabatic free energies of reaction and accounts for the orbitals relaxation

$$\lambda = \Delta E_{ET} - \Delta G^0_{ET} \tag{27}$$

The reaction rate constants (k) can be calculated using the conventional transition state theory (TST) which is one of the most robust theoretical methodologies for this purpose, requiring only structural, energy, and vibrational frequency information for reactants and transition states, allowing it to be applied to a wide range of chemical processes.[256−258] Despite its simplicity, it has been shown to reproduce fine the experimentally measured data on free radicals scavenging kinetics.[82,84,96,129] It is computed usually in the framework of 1 M standard state[258] using the Eyring equation (eq 28)

$$k^{TST} = \frac{k_B T}{h} e^{-\Delta G^{\neq}/RT} \tag{28}$$

where k_B and h are the Boltzmann and Planck constants, respectively. $\Delta G^{\ddagger}$ is the free energy of activation, calculated as the difference in energies between transition state and reactants, while R and T denote the gas constant and temperature, respectively.

The more sophisticated Eckart approach,[259] also known as the zero-tunneling method, employs the Boltzmann average of the ratio of quantum and classical probabilities[260] and is suggested for processes in which reactants are transformed into products over energy barriers. Such processes include the HAT reaction, which involves the motion of a light particle (here $H^\bullet$) that can easily tunnel, as well as some RAF pathways. Tunneling corrections ($\kappa(T)$), also known in the literature as transmission coefficients ($\gamma(T)$), are included, as is reaction path degeneracy (σ). $\kappa(T)$ can significantly modulate reaction rate values between relatively similar reacting species, such as $CH_3OO^\bullet$ or $OOH^\bullet$.[118] It can be estimated using external software, for example Eyringpy.[261] The number of identical reaction paths, on the other hand, is reflected by σ and can be calculated by labeling all similar atoms and counting the number of different but equivalent configurations that can be formed by rotating, but not reflecting them. They can also be established using the Pollak and Pechukas[262] scheme (Table 5). Taking everything into account, eq 29 is obtained

$$k^{TST} = \sigma\kappa(T)\frac{k_B T}{h} e^{-\Delta G^{\neq}/RT} \tag{29}$$

Table 5. Point Groups and the Reaction Path Degeneracy Values That Correspond to Them

Point group	σ	Point group	σ
C_1	1	D_{3h}	6
C_s	1	D_{5h}	10
C_2	2	$D_{\infty h}$	2
C_{2v}	2	D_{3d}	6
C_{3v}	3	T_d	12
$C_{\infty v}$	1	O_h	24
D_{2h}	4		

As previously stated, radicals with high reactivity often react at diffusion-limited rates ($k \geq 10^8\ M^{-1}\ s^{-1}$) with the vast majority of chemical compounds. For an irreversible bimolecular diffusion-controlled reaction, the Collins−Kimball theory,[263] in conjunction with the steady-state Smoluchowski rate constant[264] and the Stokes−Einstein approaches,[265] must be used to calculate rate constants properly (Table 6). They are frequently applied in case of RAF mechanisms, which is not surprising given that these types of radical attacks usually occur in the absence of energy barriers, making it difficult to localize the transition state.[82]

The total reaction rate constant values (k^{TOT}) for all acid−base species (i) present at the specified pH multiplied by the corresponding molar fractions (f) allow the overall reaction rate constant ($k^{overall}$), which corresponds to the empirically observed reaction rate, to be calculated

$$k^{overall} = \sum_{i=\{species\}} f(i)k^{TOT}(i) \tag{30}$$

The reaction rate constants for each antioxidative mechanism (j) are then added to calculate the k^{TOT} values for all acid−base species

$$k^{TOT} = \sum_{j=\{mechanism\}} k^{mech}(j) \tag{31}$$

The k^{mech} (eq 32) is defined as the sum of reaction rate constants (k^{TST} or k^{app}, depending on the kinetic model used, here simply represented by k) from to the same antioxidative mechanism but calculated at different reaction sites (l)

https://doi.org/10.1021/acs.jcim.2c00104
J. Chem. Inf. Model. 2022, 62, 2639−2658

Table 6. Collins–Kimball Theory, Steady-State Smoluchowski, and Stokes–Einstein Equation Mathematical Formulations

Name	Related formula	Variables
Collins–Kimball theory	$k^{app} = \frac{k^{D}k^{TST}}{k^{D} + k^{TST}}$	k_{app}: apparent rate constant
Steady-state Smoluchowski	$k^{D} = 4\pi R D_{AB} N_A$	k^{D}: steady-state Smoluchowski k^{TST}: thermal rate constant (obtained from TST) R: reaction distance N_A: Avogadro number D_{AB}: mutual diffusion coefficient of the reactants A (free radical) and B (antioxidant)
Stokes–Einstein equation	$D_{A\text{ or }B} = \frac{k_B T}{6\pi\eta r_{A\text{ or }B}}$	k_B: Boltzmann constant T: temperature η: viscosity of solvent r: radius of solute

$$k^{mech} = \sum_{l=\{pathway\}} k(l) \tag{32}$$

The branching ratio ($\Gamma(l)$), (eq 33) can be used to calculate the percentage contribution of an antioxidative pathway (l) to the total reaction rate (l) using the following formula

$$\Gamma(l) = \frac{k(l)}{k^{overall}} \tag{33}$$

Furthermore, the relative antioxidative activity of the examined molecule can be calculated by dividing its $k^{overall}$ by the $k^{overall}$ of ref 45 (e.g., Trolox, Tx) as presented in eq 34

$$r^{T} = \frac{k^{overall}}{k_{Tx}^{overall}} \tag{34}$$

A threshold of $k^{overall} = 1.2 \times 10^3\ M^{-1}\ s^{-1}$ was proposed for quantifying antioxidant activity as a value close to the rate constant of the interaction between $HOO^{\bullet}$ and polyunsaturated fatty acids[3,21,126]. Compounds with higher $k^{overall}$ values are thought to be effective antioxidants, while those with lower are thought to be ineffective.

Thermochemistry and Kinetic Ensemble. Galano, Alvarez-Idaboy and coworkers combined the above considerations into the quantum mechanics-based test for overall free radical scavenging activity (QM-ORSA) protocol,[3,154,266] which is proposed as a feasible tool to assess radical scavenging activity in physiologically relevant solvents. It entails the impact of all existing acid–base forms, identifying RAF, HAT, and SET mechanisms viability, and then subjecting them to kinetic analysis. This method has been already used successfully in numerous papers.[41,45,58,69,82,88,104,118]

CONCLUDING REMARKS AND ADDITIONAL CONSIDERATIONS

Antioxidants were and are extensively studied using computational quantum chemistry. A number of useful tools are developed to provide insight into their electronic structure and reactivity. Importantly, scientists are not limited in their research to already known procedures but continously suggest new ones and apply them in their research. Therefore, each paper proposes some novel techniques in this matter, as well as new conclusions that provide greater insight into the chemistry of the antioxidants that have been already studied or projected from the scratch. As previously stated, because all antioxidants tend to exhibit similar patterns of activity, they can all be examined in the same way, whether we are talking about fullerenes, natural plant products, or entirely newly synthesized structures.

Certain points, however, should be reconsidered or reinterpreted:

- Almost all of the research considered reactive oxygen species, with only a minor focus on radicals containing nitrogen, carbon, and sulfur elements. These are known to be linked to oxidative stress,[267−269] so research into them would fill the gap.
- When discussing *in vivo* activity, although solvation effects and hence deprotonation are considered, the importance of metabolites should be emphasized. The gut microbiota are the first to alter antioxidant structure, influencing primarily their absorption profile. They are then metabolized in the liver, where they undergo further changes that result in products with vastly different activity. By focusing solely on generic structures the outcomes are indeed limited to *in vitro* results, casting doubt on the physiological activities as free radicals scavengers, capable of halting the development of oxidative stress and resulting diseases.
- The dual nature of free radicals extends to the products derived from the antioxidants. Castañeda-Arriaga et al.[102] discussed possible prooxidant behavior of such, in which the new forms may still be capable of oxidizing biologically relevant structures. The authors also proposed them to be able to self-regenerate, allowing them to work multiple times. This fresh topic appears to be a relevant aspect that needs to be considered when attempting to prove experimental observations.

DATA AND SOFTWARE AVAILABILITY

Multiwfn (current version 3.7) is a free, open-source software developed by Tian Lu for wave function analysis and visualization. It is available for download at http://sobereva.com/multiwfn/. Eyring.py (current version 2.0) is a Python-based program developed by the Merino et al. group for computing rate constants of unimolecular or bimolecular reactions in the gas phase and in solution using transition state theory. For that purpose, it takes into account reaction symmetry, tunneling corrections, Collins–Kimball theory, Marcus theory, and species molar fractions. It is available at

https://doi.org/10.1021/acs.jcim.2c00104
J. Chem. Inf. Model. 2022, 62, 2639−2658

https://www.theochemmerida.org/eyringpy. GROMACS (current version 2021.5) is a free package, available under a LGPL license, created to perform molecular dynamics of proteins, lipids, nucleic acids as well as nonbiological systems. It is accessible from http://www.gromacs.org. Amber (current version 20) is a paid versatile suite of biomolecular simulation programs. It can be found at https://ambermd.org/index.php. CHARMM is a molecular simulation program that uses enhanced sampling methods and multiscale techniques to study many-particle systems. For academic users, the version "charmm" is free. The software is available for free download at https://academiccharmm.org.

AUTHOR INFORMATION

Corresponding Author

Maciej Spiegel − *Department of Pharmacognosy and Herbal Medicines, Wroclaw Medical University, 50-556 Wroclaw, Poland;* orcid.org/0000-0002-8012-1026; Email: maciej.spiegel@student.umed.wroc.pl

Complete contact information is available at: https://pubs.acs.org/10.1021/acs.jcim.2c00104

Notes

The author declares no competing financial interest.

REFERENCES

(1) Valko, M.; Leibfritz, D.; Moncol, J.; Cronin, M. T. D.; Mazur, M.; Telser, J. Free Radicals and Antioxidants in Normal Physiological Functions and Human Disease. *Int. J. Biochem. Cell Biol.* **2007**, *39* (1), 44−84.

(2) Ames, B. N.; Shigenaga, M. K.; Hagen, T. M. Oxidants, antioxidants, and the degenerative diseases of aging. *Proc. Natl. Acad. Sci. U.S.A.* **1993**, *90* (17), 7915−7922.

(3) Galano, A.; Alvarez-Idaboy, J. R. Computational Strategies for Predicting Free Radical Scavengers' Protection against Oxidative Stress: Where Are We and What Might Follow? *Int. J. Quantum Chem.* **2019**, *119* (2), No. e25665.

(4) Kumar, N.; Goel, N. Phenolic Acids: Natural Versatile Molecules with Promising Therapeutic Applications. *Biotechnol. Reports* **2019**, *24*, No. e00370.

(5) Sisa, M.; Bonnet, S. L.; Ferreira, D.; Van Der Westhuizen, J. H. Photochemistry of Flavonoids. *Molecules* **2010**, *15* (8), 5196−5245.

(6) Miguel, M. G. Betalains in Some Species of the Amaranthaceae Family: A Review. *Antioxidants* **2018**, *7* (4), 53.

(7) Reygaert, W. C. Green Tea Catechins: Their Use in Treating and Preventing Infectious Diseases. *Biomed Res. Int.* **2018**, *2018*, 1−9.

(8) Ross, S. A.; Ziska, D. S.; Zhao, K.; ElSohly, M. A. Variance of Common Flavonoids by Brand of Grapefruit Juice. *Fitoterapia* **2000**, *71* (2), 154−161.

(9) Ma, Y.; Feng, Y.; Diao, T.; Zeng, W.; Zuo, Y. Experimental and Theoretical Study on Antioxidant Activity of the Four Anthocyanins. *J. Mol. Struct.* **2020**, *1204*, 127509.

(10) Spiegel, M.; Andruniów, T.; Sroka, Z. Flavones' and Flavonols' Antiradical Structure- Activity Relationship—a Quantum Chemical Study. *Antioxidants* **2020**, *9* (6), 461.

(11) Ali, H. M.; Ali, I. H. Structure-Antioxidant Activity Relationships, QSAR, DFT Calculation, and Mechanisms of Flavones and Flavonols. *Med. Chem. Res.* **2019**, *28* (12), 2262−2269.

(12) Mendes, R. A.; Almeida, S. K. C.; Soares, I. N.; Barboza, C. A.; Freitas, R. G.; Brown, A.; de Souza, G. L. C. Evaluation of the Antioxidant Potential of Myricetin 3-O-α-L-Rhamnopyranoside and Myricetin 4′-O-α-L-Rhamnopyranoside through a Computational Study. *J. Mol. Model.* **2019**, *25* (4), 89.

(13) Maciel, E. N.; Soares, I. N.; da Silva, S. C.; de Souza, G. L. C. A Computational Study on the Reaction between Fisetin and 2,2-Diphenyl-1-Picrylhydrazyl (DPPH). *J. Mol. Model.* **2019**, *25* (4), 103.

(14) Yi, Y.; Adrjan, B.; Li, J.; Hu, B.; Roszak, S. NMR Studies of Daidzein and Puerarin: Active Anti-Oxidants in Traditional Chinese Medicine. *J. Mol. Model.* **2019**, *25* (7), 202.

(15) Song, X.; Wang, Y.; Gao, L. Mechanism of Antioxidant Properties of Quercetin and Quercetin-DNA Complex. *J. Mol. Model.* **2020**, *26* (6), 133.

(16) Son, N. T.; Mai Thanh, D. T.; Van Trang, N. Flavone Norartocarpetin and Isoflavone 2′-Hydroxygenistein: A Spectroscopic Study for Structure, Electronic Property and Antioxidant Potential Using DFT (Density Functional Theory). *J. Mol. Struct.* **2019**, *1193*, 76−88.

(17) Zheng, Y. Z.; Deng, G.; Guo, R.; Fu, Z. M.; Chen, D. F. Theoretical Insight into the Antioxidative Activity of Isoflavonoid: The Effect of the C2 = C3 Double Bond. *Phytochemistry* **2019**, *166*, 112075.

(18) Biela, M.; Rimarčík, J.; Senajová, E.; Kleinová, A.; Klein, E. Antioxidant Action of Deprotonated Flavonoids: Thermodynamics of Sequential Proton-Loss Electron-Transfer. *Phytochemistry* **2020**, *180*, 112528.

(19) Anitha, S.; Krishnan, S.; Senthilkumar, K.; Sasirekha, V. Theoretical Investigation on the Structure and Antioxidant Activity of (+) Catechin and (−) Epicatechin-a Comparative Study. *Mol. Phys.* **2020**, *118* (17), e1745917.

(20) Ninh The, S.; Do Minh, T.; Nguyen Van, T. Isoflavones and Isoflavone Glycosides: Structural-Electronic Properties and Antioxidant Relations-A Case of DFT Study. *J. Chem.* **2019**, *2019* (d), 1.

(21) Vásquez-Espinal, A.; Yañez, O.; Osorio, E.; Areche, C.; García-Beltrán, O.; Ruiz, L. M.; Cassels, B. K.; Tiznado, W. Theoretical Study of the Antioxidant Activity of Quercetin Oxidation Products. *Front. Chem.* **2019**, *7*, 1−10.

(22) Zheng, Y. Z.; Deng, G.; Guo, R.; Chen, D. F.; Fu, Z. M. Substituent Effects on the Radical Scavenging Activity of Isoflavonoid. *Int. J. Mol. Sci.* **2019**, *20* (2), 397.

(23) Zheng, Y. Z.; Deng, G.; Guo, R.; Chen, D. F.; Fu, Z. M. DFT Studies on the Antioxidant Activity of Naringenin and Its Derivatives: Effects of the Substituents at C3. *Int. J. Mol. Sci.* **2019**, *20* (6), 1450.

(24) Žuvela, P.; David, J.; Yang, X.; Huang, D.; Wong, M. W. Non-Linear Quantitative Structure-Activity Relationships Modelling, Mechanistic Study and in-Silico Design of Flavonoids as Potent Antioxidants. *Int. J. Mol. Sci.* **2019**, *20* (9), 2328.

(25) Xu, Y.; Qian, L. L.; Yang, J.; Han, R. M.; Zhang, J. P.; Skibsted, L. H. Kaempferol Binding to Zinc(II), Efficient Radical Scavenging through Increased Phenol Acidity. *J. Phys. Chem. B* **2018**, *122* (44), 10108−10117.

(26) Mendes, R. A.; Almeida, S. K. C.; Soares, I. N.; Barboza, C. A.; Freitas, R. G.; Brown, A.; de Souza, G. L. C. A Computational Investigation on the Antioxidant Potential of Myricetin 3,4′-Di-O-α-L-Rhamnopyranoside. *J. Mol. Model.* **2018**, *24* (6), 133.

(27) Rajan, V. K.; Shameera Ahamed, T. K.; Muraleedharan, K. Studies on the UV Filtering and Radical Scavenging Capacity of the Bitter Masking Flavanone Eriodictyol. *J. Photochem. Photobiol. B Biol.* **2018**, *185* (June), 254−261.

(28) Son, N. T.; Thuy, P. T.; Van Trang, N. Antioxidative Capacities of Stilbenoid Suaveolensone A and Flavonoid Suaveolensone B: A Detailed Analysis of Structural-Electronic Properties and Mechanisms. *J. Mol. Struct.* **2021**, *1224*, 129025.

(29) Tiwari, M. K.; Mishra, P. C. Scavenging of Hydroxyl, Methoxy, and Nitrogen Dioxide Free Radicals by Some Methylated Isoflavones. *J. Mol. Model.* **2018**, *24* (10), 287.

(30) Zhou, H.; Li, X.; Shang, Y.; Chen, K. Radical Scavenging Activity of Puerarin: A Theoretical Study. *Antioxidants* **2019**, *8* (12), 590.

(31) Thong, N. M.; Vo, Q. V.; Huyen, T. L.; Bay, M. V.; Tuan, D.; Nam, P. C. Theoretical Study for Exploring the Diglycoside Substituent Effect on the Antioxidative Capability of Isorhamnetin Extracted from Anoectochilus Roxburghii. *ACS Omega* **2019**, *4* (12), 14996−15003.

(32) Zheng, Y. Z.; Chen, D. F.; Deng, G.; Guo, R. The Substituent Effect on the Radical Scavenging Activity of Apigenin. *Molecules* **2018**, *23* (8), 1989.

(33) Li, Z.; Moalin, M.; Zhang, M.; Vervoort, L.; Hursel, E.; Mommers, A.; Haenen, G. R. M. M. The Flow of the Redox Energy in

Quercetin during Its Antioxidant Activity in Water. *Int. J. Mol. Sci.* **2020**, *21* (17), 6015.
(34) Milenkovic, D.; Dimitric Markovic, J. M; Dimic, D.; Jeremic, S.; Amic, D.; Stanojevic Pirkovic, M.; Markovic, Z. S Structural Characterization of Kaempferol: A Spectroscopic and Computational Study. *Maced. J. Chem. Chem. Eng.* **2019**, *38* (1), 49−62.
(35) Manrique-de-la-Cuba, M. F.; Gamero-Begazo, P.; Valencia, D. E.; Barazorda-Ccahuana, H. L.; Gómez, B. Theoretical Study of the Antioxidant Capacity of the Flavonoids Present in the Annona Muricata (Soursop) Leaves. *J. Mol. Model.* **2019**, *25* (7), 200.
(36) Castañeda-Arriaga, R.; Marino, T.; Russo, N.; Alvarez-Idaboy, J. R.; Galano, A. Chalcogen Effects on the Primary Antioxidant Activity of Chrysin and Quercetin. *New J. Chem.* **2020**, *44* (21), 9073−9082.
(37) Heřmánková, E.; Zatloukalová, M.; Biler, M.; Sokolová, R.; Bancířová, M.; Tzakos, A. G.; Křen, V.; Kuzma, M.; Trouillas, P.; Vacek, J. Redox Properties of Individual Quercetin Moieties. *Free Radic. Biol. Med.* **2019**, *143*, 240−251.
(38) Milenković, D.; Đorović, J.; Petrović, V.; Avdović, E.; Marković, Z. Hydrogen Atom Transfer versus Proton Coupled Electron Transfer Mechanism of Gallic Acid with Different Peroxy Radicals. *React. Kinet. Mech. Catal.* **2018**, *123* (1), 215−230.
(39) Amić, A.; Marković, Z.; Dimitrić Marković, J. M.; Milenković, D.; Stepanić, V. Antioxidative Potential of Ferulic Acid Phenoxyl Radical. *Phytochemistry* **2020**, *170*, 112218.
(40) Vo, Q. V.; Bay, M. V.; Nam, P. C.; Quang, D. T.; Flavel, M.; Hoa, N. T.; Mechler, A. Theoretical and Experimental Studies of the Antioxidant and Antinitrosant Activity of Syringic Acid. *J. Org. Chem.* **2020**, *85* (23), 15514−15520.
(41) Medina, M. E.; Galano, A.; Trigos, Á. Scavenging Ability of Homogentisic Acid and Ergosterol toward Free Radicals Derived from Ethanol Consumption. *J. Phys. Chem. B* **2018**, *122* (30), 7514−7521.
(42) Kalinowska, M.; Sienkiewicz-Gromiuk, J.; Świderski, G.; Pietryczuk, A.; Cudowski, A.; Lewandowski, W. Zn(II) Complex of Plant Phenolic Chlorogenic Acid: Antioxidant, Antimicrobial and Structural Studies. *Materials (Basel).* **2020**, *13* (17), 3745.
(43) Spiegel, M.; Kapusta, K.; Kołodziejczyk, W.; Saloni, J.; Żbikowska, B.; Hill, G. A.; Sroka, Z. Antioxidant Activity of Selected Phenolic Acids-Ferric Reducing Antioxidant Power Assay and QSAR Analysis of the Structural Features. *Molecules* **2020**, *25* (13), 3088.
(44) Zheng, Y. Z.; Fu, Z. M.; Deng, G.; Guo, R.; Chen, D. F. Free Radical Scavenging Potency of Ellagic Acid and Its Derivatives in Multiple H+/E- Processes. *Phytochemistry* **2020**, *180* (July), 112517.
(45) Tošović, J.; Bren, U. Antioxidative Action of Ellagic Acid—A Kinetic DFT Study. *Antioxidants* **2020**, *9* (7), 587.
(46) Reina, M.; Guzmán-López, E. G.; Romeo, I.; Marino, T.; Russo, N.; Galano, A. Computationally Designed: P -Coumaric Acid Analogs: Searching for Neuroprotective Antioxidants. *New J. Chem.* **2021**, *45* (32), 14369−14380.
(47) Chen, J.; Yang, J.; Ma, L.; Li, J.; Shahzad, N.; Kim, C. K. Structure-Antioxidant Activity Relationship of Methoxy, Phenolic Hydroxyl, and Carboxylic Acid Groups of Phenolic Acids. *Sci. Rep.* **2020**, *10* (1), 2611.
(48) Vo, Q. V.; Nam, P. C.; Bay, M. V.; Thong, N. M.; Cuong, N. D.; Mechler, A. Density Functional Theory Study of the Role of Benzylic Hydrogen Atoms in the Antioxidant Properties of Lignans. *Sci. Rep.* **2018**, *8* (1), 1−10.
(49) Xue, Y.; Liu, Y.; Zhang, L.; Wang, H.; Luo, Q.; Chen, R.; Liu, Y.; Li, Y. Antioxidant and Spectral Properties of Chalcones and Analogous Aurones: Theoretical Insights. *Int. J. Quantum Chem.* **2019**, *119* (3), e25808.
(50) Boulebd, H. The Role of Benzylic-Allylic Hydrogen Atoms on the Antiradical Activity of Prenylated Natural Chalcones: A Thermodynamic and Kinetic Study. *J. Biomol. Struct. Dyn.* **2021**, *39* (6), 1955−1964.
(51) Xue, Y.; Liu, Y.; Xie, Y.; Cong, C.; Wang, G.; An, L.; Teng, Y.; Chen, M.; Zhang, L. Antioxidant Activity and Mechanism of Dihydrochalcone C-Glycosides: Effects of C-Glycosylation and Hydroxyl Groups. *Phytochemistry* **2020**, *179* (April), 112393.
(52) Llano, S.; Gómez, S.; Londoño, J.; Restrepo, A. Antioxidant Activity of Curcuminoids. *Phys. Chem. Chem. Phys.* **2019**, *21* (7), 3752−3760.
(53) Li, Y.; Toscano, M.; Mazzone, G.; Russo, N. Antioxidant Properties and Free Radical Scavenging Mechanisms of Cyclocurcumin. *New J. Chem.* **2018**, *42* (15), 12698−12705.
(54) Ali, H. M.; Ali, I. H. Energetic and Electronic Computation of the Two-Hydrogen Atom Donation Process in Catecholic and Non-Catecholic Anthocyanidins. *Food Chem.* **2018**, *243*, 145−150.
(55) Chen, B.; Ma, Y.; Li, H.; Chen, X.; Zhang, C.; Wang, H.; Deng, Z. The Antioxidant Activity and Active Sites of Delphinidin and Petunidin Measured by DFT, in Vitro Chemical-Based and Cell-Based Assays. *J. Food Biochem.* **2019**, *43* (9), 1−11.
(56) Rajan, V. K.; Hasna, C. K. K.; Muraleedharan, K. The Natural Food Colorant Peonidin from Cranberries as a Potential Radical Scavenger - A DFT Based Mechanistic Analysis. *Food Chem.* **2018**, *262*, 184−190.
(57) Shang, Y.; Zhou, H.; Li, X.; Zhou, J.; Chen, K. Theoretical Studies on the Antioxidant Activity of Viniferifuran. *New J. Chem.* **2019**, *43* (39), 15736−15742.
(58) Vo, Q. V.; Cam Nam, P.; Bay, M. V.; Minh Thong, N.; Hieu, L. T.; Mechler, A. A Theoretical Study of the Radical Scavenging Activity of Natural Stilbenes. *RSC Adv.* **2019**, *9* (72), 42020−42028.
(59) Zheng, Y. Z.; Chen, D. F.; Deng, G.; Guo, R.; Fu, Z. M. The Antioxidative Activity of Piceatannol and Its Different Derivatives: Antioxidative Mechanism Analysis. *Phytochemistry* **2018**, *156* (May), 184−192.
(60) Santos, J. L. F.; Kauffmann, A. C.; da Silva, S. C.; Silva, V. C. P.; de Souza, G. L. C. Probing Structural Properties and Antioxidant Activity Mechanisms for Eleocarpanthraquinone. *J. Mol. Model.* **2020**, *26* (9), 233.
(61) Reza Nazifi, S. M.; Asgharshamsi, M. H.; Dehkordi, M. M.; Zborowski, K. K. Antioxidant Properties of Aloe Vera Components: A DFT Theoretical Evaluation. *Free Radic. Res.* **2019**, *53* (8), 922−931.
(62) Ngo Nyobe, J. C.; Eyia Andiga, L. G.; Mama, D. B.; Ateba Amana, B.; Zobo Mfomo, J.; Flavien Aristide Alfred, T.; Ndom, J. C. A DFT Analysis on Antioxidant and Antiradical Activities from Anthraquinones Isolated from the Cameroonian Flora. *J. Chem.* **2019**, *2019*, 1.
(63) Dorović, J.; Antonijević, M.; Marković, Z. Antioxidative and Inhibition Potency of Cynodontin. *J. Serbian Soc. Comput. Mech.* **2020**, *70*, 59−70.
(64) Vega-Hissi, E. G.; Andrada, M. F.; Díaz, M. G.; Garro Martinez, J. C. Computational Study of the Hydrogen Peroxide Scavenging Mechanism of Allyl Methyl Disulfide, an Antioxidant Compound from Garlic. *Mol. Divers.* **2019**, *23* (4), 985−995.
(65) Tiwari, M. K.; Jena, N. R.; Mishra, P. C. Mechanisms of Scavenging Superoxide, Hydroxyl, Nitrogen Dioxide and Methoxy Radicals by Allicin: Catalytic Role of Superoxide Dismutase in Scavenging Superoxide Radical. *J. Chem. Sci.* **2018**, *130* (8), 1−17.
(66) Cortes, N.; Castañeda, C.; Osorio, E. H.; Cardona-Gomez, G. P.; Osorio, E. Amaryllidaceae Alkaloids as Agents with Protective Effects against Oxidative Neural Cell Injury. *Life Sci.* **2018**, *203*, 54−65.
(67) Dung, N. T.; Thanh, D. M.; Huong, N. T.; Thuy, P. T.; Hoan, N. T.; Thanh, D. T. M.; Van Trang, N.; Son, N. T. Quinolone and Isoquinolone Alkaloids: The Structural-Electronic Effects and the Antioxidant Mechanisms. *Struct. Chem.* **2020**, *31* (6), 2435−2450.
(68) Boulebd, H. Are Thymol, Rosefuran, Terpinolene and Umbelliferone Good Scavengers of Peroxyl Radicals? *Phytochemistry* **2021**, *184*, 112670.
(69) Vo, Q. V.; Tam, N. M.; Hieu, L. T.; Van Bay, M.; Thong, N. M.; Le Huyen, T.; Hoa, N. T.; Mechler, A. The Antioxidant Activity of Natural Diterpenes: Theoretical Insights. *RSC Adv.* **2020**, *10* (25), 14937−14943.
(70) Boulebd, H. DFT Study of the Antiradical Properties of Some Aromatic Compounds Derived from Antioxidant Essential Oils: C-H Bond vs. O-H Bond. *Free Radic. Res.* **2019**, *53* (11−12), 1125−1134.
(71) Hernandez, D. A.; Tenorio, F. J. Reactivity Indexes of Antioxidant Molecules from Rosmarinus Officinalis. *Struct. Chem.* **2018**, *29* (3), 741−751.

https://doi.org/10.1021/acs.jcim.2c00104
J. Chem. Inf. Model. 2022, 62, 2639−2658

(72) Ngo, T. C.; Nguyen, T. H.; Dao, D. Q. Radical Scavenging Activity of Natural-Based Cassaine Diterpenoid Amides and Amines. *J. Chem. Inf. Model.* **2019**, *59* (2), 766−776.
(73) Romeo, I.; Parise, A.; Galano, A.; Russo, N.; Alvarez-Idaboy, J. R.; Marino, T. The Antioxidant Capability of Higenamine: Insights from Theory. *Antioxidants* **2020**, *9* (5), 358.
(74) Boulebd, H. Theoretical Insights into the Antioxidant Activity of Moracin T. *Free Radic. Res.* **2020**, *54* (4), 221−230.
(75) Dao, D. Q.; Phan, T. T. T.; Nguyen, T. L. A.; Trinh, P. T. H.; Tran, T. T. V.; Lee, J. S.; Shin, H. J.; Choi, B.-K. Insight into Antioxidant and Photoprotective Properties of Natural Compounds from Marine Fungus. *J. Chem. Inf. Model.* **2020**, *60* (3), 1329−1351.
(76) Elshamy, A. I.; Yoneyama, T.; Trang, N. V.; Son, N. T.; Okamoto, Y.; Ban, S.; Noji, M.; Umeyama, A. A New Cerebroside from the Entomopathogenic Fungus Ophiocordyceps Longiissima: Structural-Electronic and Antioxidant Relations. Experimental and DFT Calculated Studies. *J. Mol. Struct.* **2020**, *1200*, 127061.
(77) Dávalos, J. Z.; Valderrama-Negrón, A. C.; Barrios, J. R.; Freitas, V. L. S.; Ribeiro Da Silva, M. D. M. C. Energetic and Structural Properties of Two Phenolic Antioxidants: Tyrosol and Hydroxytyrosol. *J. Phys. Chem. A* **2018**, *122* (16), 4130−4137.
(78) Montero, G.; Arriagada, F.; Günther, G.; Bollo, S.; Mura, F.; Berríos, E.; Morales, J. Phytoestrogen Coumestrol: Antioxidant Capacity and Its Loading in Albumin Nanoparticles. *Int. J. Pharm.* **2019**, *562*, 86−95.
(79) Shameera Ahamed, T. K.; Rajan, V. K.; Sabira, K.; Muraleedharan, K. DFT and QTAIM Based Investigation on the Structure and Antioxidant Behavior of Lichen Substances Atranorin, Evernic Acid and Diffractaic Acid. *Comput. Biol. Chem.* **2019**, *80*, 66−78.
(80) Wang, A.; Lu, Y.; Du, X.; Shi, P.; Zhang, H. A Theoretical Study on the Antioxidant Activity of Uralenol and Neouralenol Scavenging Two Radicals. *Struct. Chem.* **2018**, *29* (4), 1067−1075.
(81) Zhang, D.; Wang, C.; Shen, L.; Shin, H. C.; Lee, K. B.; Ji, B. Comparative Analysis of Oxidative Mechanisms of Phloroglucinol and Dieckol by Electrochemical, Spectroscopic, Cellular and Computational Methods. *RSC Adv.* **2018**, *8* (4), 1963−1972.
(82) Parise, A.; De Simone, B. C.; Marino, T.; Toscano, M.; Russo, N. Quantum Mechanical Predictions of the Antioxidant Capability of Moracin C Isomers. *Front. Chem.* **2021**, *9* (April), 1−9.
(83) Gonçalves, L. C. P.; Lopes, N. B.; Augusto, F. A.; Pioli, R. M.; Machado, C. O.; Freitas-Dörr, B. C.; Suffredini, H. B.; Bastos, E. L. Phenolic Betalain as Antioxidants: Meta Means More. *Pure Appl. Chem.* **2020**, *92* (2), 243−253.
(84) Perez-Gonzalez, A.; Prejano, M.; Russo, N.; Marino, T.; Galano, A. Capsaicin, a Powerful •OH-Inactivating Ligand. *Antioxidants* **2020**, *9* (12), 1247.
(85) Spiegel, M.; Gamian, A.; Sroka, Z. Antiradical Activity of Beetroot (Beta Vulgaris L.) Betalains. *Molecules* **2021**, *26* (9), 2439.
(86) Nakashima, K. K.; Bastos, E. L. Rationale on the High Radical Scavenging Capacity of Betalains. *Antioxidants* **2019**, *8* (7), 222.
(87) Tabrizi, L.; Dao, D. Q.; Vu, T. A. Experimental and Theoretical Evaluation on the Antioxidant Activity of a Copper(Ii) Complex Based on Lidocaine and Ibuprofen Amide-Phenanthroline Agents. *RSC Adv.* **2019**, *9* (6), 3320−3335.
(88) Boulebd, H.; Tam, N. M.; Mechler, A.; Vo, Q. V. Substitution Effects on the Antiradical Activity of Hydralazine: A DFT Analysis. *New J. Chem.* **2020**, *44* (38), 16577−16583.
(89) Minnelli, C.; Laudadio, E.; Galeazzi, R.; Rusciano, D.; Armeni, T.; Stipa, P.; Cantarini, M.; Mobbili, G. Synthesis, Characterization and Antioxidant Properties of a New Lipophilic Derivative of Edaravone. *Antioxidants* **2019**, *8* (8), 258.
(90) Bortoli, M.; Dalla Tiezza, M.; Muraro, C.; Pavan, C.; Ribaudo, G.; Rodighiero, A.; Tubaro, C.; Zagotto, G.; Orian, L. Psychiatric Disorders and Oxidative Injury: Antioxidant Effects of Zolpidem Therapy Disclosed In Silico. *Comput. Struct. Biotechnol. J.* **2019**, *17*, 311−318.
(91) Boulebd, H.; Khodja, I. A.; Bay, M. V.; Hoa, N. T.; Mechler, A.; Vo, Q. V. Thermodynamic and Kinetic Studies of the Radical Scavenging Behavior of Hydralazine and Dihydralazine: Theoretical Insights. *J. Phys. Chem. B* **2020**, *124* (20), 4123−4131.
(92) Muraro, C.; Dalla Tiezza, M.; Pavan, C.; Ribaudo, G.; Zagotto, G.; Orian, L. Major Depressive Disorder and Oxidative Stress: In Silico Investigation of Fluoxetine Activity against ROS. *Appl. Sci.* **2019**, *9* (17), 3631.
(93) Purushothaman, A.; Sheeja, A. A.; Janardanan, D. Hydroxyl Radical Scavenging Activity of Melatonin and Its Related Indolamines. *Free Radic. Res.* **2020**, *54* (5), 373−383.
(94) Baj, A.; Cedrowski, J.; Olchowik-Grabarek, E.; Ratkiewicz, A.; Witkowski, S. Synthesis, DFT Calculations, and in Vitro Antioxidant Study on Novel Carba-Analogs of Vitamin E. *Antioxidants* **2019**, *8* (12), 589.
(95) Pandithavidana, D. R.; Jayawardana, S. B. Comparative Study of Antioxidant Potential of Selected Dietary Vitamins; Computational Insights. *Molecules* **2019**, *24* (9), 1646.
(96) Ardjani, T. E. A.; Alvarez-Idaboy, J. R. Radical Scavenging Activity of Ascorbic Acid Analogs: Kinetics and Mechanisms. *Theor. Chem. Acc.* **2018**, *137* (5), na DOI: 10.1007/s00214-018-2252-x.
(97) Bentz, E. N.; Lobayan, R. M.; Martínez, H.; Redondo, P.; Largo, A. Intrinsic Antioxidant Potential of the Aminoindole Structure: A Computational Kinetics Study of Tryptamine. *J. Phys. Chem. B* **2018**, *122* (24), 6386−6395.
(98) Dimic, D.; Milenkovic, D.; Markovic, Z.; Dimitric-Markovic, J. The Reactivity of Dopamine Precursors and Metabolites towards ABTS● -: An Experimental and Theoretical Study. *J. Serbian Chem. Soc.* **2019**, *84* (8), 877−889.
(99) Jabeen, H.; Saleemi, S.; Razzaq, H.; Yaqub, A.; Shakoor, S.; Qureshi, R. Investigating the Scavenging of Reactive Oxygen Species by Antioxidants via Theoretical and Experimental Methods. *J. Photochem. Photobiol. B Biol.* **2018**, *180*, 268−275.
(100) Dimic, D.; Nakarada, Đu.; Mojovic, M.; Dimitric Markovic, J. An Experimental and Theoretical Study of the Reactivity of Selected Catecholamines and Their Precursors towards Ascorbyl Radical. *J. Serbian Soc. Comput. Mech.* **2020**, *12*, 1−12.
(101) Reina, M.; Castañeda-Arriaga, R.; Perez-Gonzalez, A.; Guzman-Lopez, E. G.; Tan, D.-X.; Reiter, R. J.; Galano, A. A Computer-Assisted Systematic Search for Melatonin Derivatives with High Potential as Antioxidants. *Melatonin Res.* **2018**, *1* (1), 27−58.
(102) Castañeda-Arriaga, R.; Pérez-González, A.; Reina, M.; Galano, A. Computer-Designed Melatonin Derivatives: Potent Peroxyl Radical Scavengers with No pro-Oxidant Behavior. *Theor. Chem. Acc.* **2020**, *139* (8), 1−12.
(103) Dimić, D.; Milenković, D.; Ilić, J.; Šmit, B.; Amić, A.; Marković, Z.; Dimitrić Marković, J. Experimental and Theoretical Elucidation of Structural and Antioxidant Properties of Vanillylmandelic Acid and Its Carboxylate Anion. *Spectrochim. Acta - Part A Mol. Biomol. Spectrosc.* **2018**, *198*, 61−70.
(104) Boulebd, H.; Mechler, A.; Hoa, N. T.; Vo, Q. V. Thermodynamic and Kinetic Studies of the Antiradical Activity of 5-Hydroxymethylfurfural: Computational Insights. *New J. Chem.* **2020**, *44* (23), 9863−9869.
(105) Reina, M.; Martínez, A. A New Free Radical Scavenging Cascade Involving Melatonin and Three of Its Metabolites (3OHM, AFMK and AMK). *Comput. Theor. Chem.* **2018**, *1123*, 111−118.
(106) Sykula, A.; Kowalska-Baron, A.; Dzeikala, A.; Bodzioch, A.; Lodyga-Chruscinska, E. An Experimental and DFT Study on Free Radical Scavenging Activity of Hesperetin Schiff Bases. *Chem. Phys.* **2019**, *517*, 91−103.
(107) Amić, A.; Marković, Z.; Klein, E.; Dimitrić Marković, J. M.; Milenković, D. Theoretical Study of the Thermodynamics of the Mechanisms Underlying Antiradical Activity of Cinnamic Acid Derivatives. *Food Chem.* **2018**, *246*, 481−489.
(108) Wang, L.; Yang, F.; Zhao, X.; Li, Y. Effects of Nitro- and Amino-Group on the Antioxidant Activity of Genistein: A Theoretical Study. *Food Chem.* **2019**, *275*, 339−345.
(109) Hernández-García, L.; Sandoval-Lira, J.; Rosete-Luna, S.; Niño-Medina, G.; Sanchez, M. Theoretical Study of Ferulic Acid Dimer

Derivatives: Bond Dissociation Enthalpy, Spin Density, and HOMO-LUMO Analysis. *Struct. Chem.* **2018**, *29* (5), 1265−1272.
(110) Zheng, Y. Z.; Zhou, Y.; Guo, R.; Fu, Z. M.; Chen, D. F. Structure-Antioxidant Activity Relationship of Ferulic Acid Derivatives: Effect of Ester Groups at the End of the Carbon Side Chain. *Lwt* **2020**, *120*, 108932.
(111) Shaikh, S. A. M.; Singh, B. G.; Barik, A.; Balaji, N. V.; Subbaraju, G. V.; Naik, D. B.; Priyadarsini, K. I. Unravelling the Effect of β-Diketo Group Modification on the Antioxidant Mechanism of Curcumin Derivatives: A Combined Experimental and DFT Approach. *J. Mol. Struct.* **2019**, *1193*, 166−176.
(112) Castro-González, L. M.; Alvarez-Idaboy, J. R.; Galano, A. Computationally Designed Sesamol Derivatives Proposed as Potent Antioxidants. *ACS Omega* **2020**, *5* (16), 9566−9575.
(113) Liu, Y.; Liu, C.; Li, J. Comparison of Vitamin c and Its Derivative Antioxidant Activity: Evaluated by Using Density Functional Theory. *ACS Omega* **2020**, *5*, 25467−25475.
(114) Stepanic, V.; Matijasic, M.; Horvat, T.; Verbanac, D.; Kucerova-Chlupacova, M.; Saso, L.; Zarkovic, N. Antioxidant Activities of Alkyl Substituted Pyrazine Derivatives of Chalcones—In Vitro and in Silico Study. *Antioxidants* **2019**, *8* (4), 90.
(115) Lauberte, L.; Fabre, G.; Ponomarenko, J.; Dizhbite, T.; Evtuguin, D. V.; Telysheva, G.; Trouillas, P. Lignin Modification Supported by DFT-Based Theoretical Study as a Way to Produce Competitive Natural Antioxidants. *Molecules* **2019**, *24* (9), 1794.
(116) Wang, G.; Liu, Y.; Zhang, L.; An, L.; Chen, R.; Liu, Y.; Luo, Q.; Li, Y.; Wang, H.; Xue, Y. Computational Study on the Antioxidant Property of Coumarin-Fused Coumarins. *Food Chem.* **2020**, *304*, 1−7.
(117) Xue, Y.; Liu, Y.; Luo, Q.; Wang, H.; Chen, R.; Liu, Y.; Li, Y. Antiradical Activity and Mechanism of Coumarin-Chalcone Hybrids: Theoretical Insights. *J. Phys. Chem. A* **2018**, *122* (43), 8520−8529.
(118) Castro-González, L. M.; Galano, A.; Alvarez-Idaboy, J. R. Free Radical Scavenging Activity of Newly Designed Sesamol Derivatives. *New J. Chem.* **2021**, *45* (27), 11960−11967.
(119) Badhani, B.; Kakkar, R. Structural, Electronic, and Reactivity Parameters of Some Triorganotin(IV) Carboxylates: A DFT Analysis. *Struct. Chem.* **2018**, *29* (3), 753−763.
(120) Tabrizi, L.; Nguyen, T. L. A.; Dao, D. Q. Experimental and Theoretical Investigation of Cyclometalated Phenylpyridine Iridium-(Iii) Complex Based on Flavonol and Ibuprofen Ligands as Potent Antioxidant. *RSC Adv.* **2019**, *9* (30), 17220−17237.
(121) Hamlaoui, I.; Bencheraiet, R.; Bensegueni, R.; Bencharif, M. Experimental and Theoretical Study on DPPH Radical Scavenging Mechanism of Some Chalcone Quinoline Derivatives. *J. Mol. Struct.* **2018**, *1156*, 385−389.
(122) Zheng, Y. Z.; Deng, G.; Chen, D. F.; Liang, Q.; Guo, R.; Fu, Z. M. Theoretical Studies on the Antioxidant Activity of Pinobanksin and Its Ester Derivatives: Effects of the Chain Length and Solvent. *Food Chem.* **2018**, *240*, 323−329.
(123) Almeida-Neto, F. W. Q.; da Silva, L. P.; Ferreira, M. K. A.; Mendes, F. R. S.; de Castro, K. K. A.; Bandeira, P. N.; de Menezes, J. E. S. A.; dos Santos, H. S.; Monteiro, N. K. V.; Marinho, E. S.; de Lima-Neto, P. Characterization of the Structural, Spectroscopic, Nonlinear Optical, Electronic Properties and Antioxidant Activity of the N-{4'-[(E)-3-(Fluorophenyl)-1-(Phenyl)-Prop-2-En-1-One]}-Acetamide. *J. Mol. Struct.* **2020**, *1220*, 128765.
(124) Milenković, D.; Avdović, E. H.; Dimić, D.; Bajin, Z.; Ristić, B.; Vuković, N.; Trifunović, S. R.; Marković, Z. S. Reactivity of the Coumarine Derivative towards Cartilage Proteins: Combined NBO, QTAIM, and Molecular Docking Study. *Monatshefte fur Chemie* **2018**, *149* (1), 159−166.
(125) Pérez-González, A.; Galano, A. On the Outstanding Antioxidant Capacity of Edaravone Derivatives through Single Electron Transfer Reactions. *J. Phys. Chem. B* **2012**, *116* (3), 1180−1188.
(126) Carreon-Gonzalez, M.; Vivier-Bunge, A.; Alvarez-Idaboy, J. R. Thiophenols, Promising Scavengers of Peroxyl Radicals: Mechanisms and Kinetics. *J. Comput. Chem.* **2019**, *40* (24), 2103−2110.
(127) Michalík, M.; Poliak, P.; Lukeš, V.; Klein, E. From Phenols to Quinones: Thermodynamics of Radical Scavenging Activity of Para-Substituted Phenols. *Phytochemistry* **2019**, *166* (June), 112077.
(128) Lee, C. Y.; Sharma, A.; Semenya, J.; Anamoah, C.; Chapman, K. N.; Barone, V. Computational Study of Ortho-Substituent Effects on Antioxidant Activities of Phenolic Dendritic Antioxidants. *Antioxidants* **2020**, *9* (3), 189.
(129) Marino, T.; Galano, A.; Mazzone, G.; Russo, N.; Alvarez-Idaboy, J. R. Chemical Insights into the Antioxidant Mechanisms of Alkylseleno and Alkyltelluro Phenols: Periodic Relatives Behaving Differently. *Chem. - A Eur. J.* **2018**, *24* (34), 8686−8691.
(130) Nakarada, Đ.; Petković, M. Mechanistic Insights on How Hydroquinone Disarms OH and OOH Radicals. *Int. J. Quantum Chem.* **2018**, *118* (4), e25496.
(131) Perin, N.; Roškarić, P.; Sović, I.; Boček, I.; Starčević, K.; Hranjec, M.; Vianello, R. Amino-Substituted Benzamide Derivatives as Promising Antioxidant Agents: A Combined Experimental and Computational Study. *Chem. Res. Toxicol.* **2018**, *31* (9), 974−984.
(132) Sheng, X. H.; Cui, C. C.; Shan, C.; Li, Y. Z.; Sheng, D. H.; Sun, B.; Chen, D. Z. O -Phenylenediamine: A Privileged Pharmacophore of Ferrostatins for Radical-Trapping Reactivity in Blocking Ferroptosis. *Org. Biomol. Chem.* **2018**, *16* (21), 3952−3960.
(133) Anastassova, N. O.; Mavrova, A. T.; Yancheva, D. Y.; Kondeva-Burdina, M. S.; Tzankova, V. I.; Stoyanov, S. S.; Shivachev, B. L.; Nikolova, R. P. Hepatotoxicity and Antioxidant Activity of Some New N,N′-Disubstituted Benzimidazole-2-Thiones, Radical Scavenging Mechanism and Structure-Activity Relationship. *Arab. J. Chem.* **2018**, *11* (3), 353−369.
(134) Orabi, E. A.; Orabi, M. A. A.; Mahross, M. H.; Abdel-Hakim, M. Computational Investigation of the Structure and Antioxidant Activity of Some Pyrazole and Pyrazolone Derivatives. *J. Saudi Chem. Soc.* **2018**, *22* (6), 705−714.
(135) Cindrić, M.; Sović, I.; Mioč, M.; Hok, L.; Boček, I.; Roškarić, P.; Butković, K.; Martin-Kleiner, I.; Starčević, K.; Vianello, R.; Kralj, M.; Hranjec, M. Experimental and Computational Study of the Antioxidative Potential of Novel Nitro and Amino Substituted Benzimidazole/Benzothiazole-2-Carboxamides with Antiproliferative Activity. *Antioxidants* **2019**, *8* (10), 477.
(136) Alisi, I. O.; Uzairu, A.; Abechi, S. E. Free Radical Scavenging Mechanism of 1,3,4-Oxadiazole Derivatives: Thermodynamics of O-H and N-H Bond Cleavage. *Heliyon* **2020**, *6* (3), No. e03683.
(137) Kumar, J.; Kumar, N.; Sati, N.; Hota, P. K. Antioxidant Properties of Ethenyl Indole: DPPH Assay and TDDFT Studies. *New J. Chem.* **2020**, *44* (21), 8960−8970.
(138) Marc, G.; Stana, A.; Oniga, S. D.; Pîrnău, A.; Vlase, L.; Oniga, O. New Phenolic Derivatives of Thiazolidine-2,4-Dione with Antioxidant and Antiradical Properties: Synthesis, Characterization, In Vitro Evaluation, and Quantum Studies. *Molecules* **2019**, *24* (11), 2060.
(139) Sonam; Chahal, V.; Kakkar, R. Theoretical Study of the Structural Features and Antioxidant Potential of 4-Thiazolidinones. *Struct. Chem.* **2020**, *31* (4), 1599−1608.
(140) Almehizia, A. A.; Abuelizz, H. A.; Taie, H. A. A.; ElHassane, A.; Marzouk, M.; Al-Salahi, R. Investigation the Antioxidant Activity of Benzo[g]Triazoloquinazolines Correlated with a DFT Study. *Saudi Pharm. J.* **2019**, *27* (1), 133−137.
(141) Al-Salahi, R.; Anouar, E. H.; Marzouk, M.; Taie, H. A. A.; Abuelizz, H. A. Screening and Evaluation of Antioxidant Activity of Some 1,2,4-Triazolo[1,5-a]Quinazoline Derivatives. *Future Med. Chem.* **2018**, *10* (4), 379−390.
(142) Bazine, I.; Cheraiet, Z.; Bensegueni, R.; Bensouici, C.; Boukhari, A. Synthesis, Antioxidant and Anticholinesterase Activities of Novel Quinoline-Aminophosphonate Derivatives. *J. Heterocycl. Chem.* **2020**, *57* (5), 2139−2149.
(143) Çakmak, E.; Özbakır Işın, D. A Theoretical Evaluation on Free Radical Scavenging Activity of 3-Styrylchromone Derivatives: The DFT Study. *J. Mol. Model.* **2020**, *26* (5), 98.
(144) Wang, Z.; Gao, X.; Zhao, Y. Mechanisms of Antioxidant Activities of Fullerenols from First-Principles Calculation. *J. Phys. Chem. A* **2018**, *122* (41), 8183−8190.

https://doi.org/10.1021/acs.jcim.2c00104
J. Chem. Inf. Model. 2022, 62, 2639−2658

(145) Orabi, E. A. Tautomerism and Antioxidant Activity of Some 4-Acylpyrazolone-Based Schiff Bases: A Theoretical Study. *RSC Adv.* **2018**, *8* (54), 30842−30850.
(146) Bakır, T.; Sayiner, H. S.; Kandemirli, F. Experimental and Theoretical Investigation of Antioxidant Activity and Capacity of Thiosemicarbazones Based on Isatin Derivatives. *Phosphorus, Sulfur Silicon Relat. Elem.* **2018**, *193* (8), 493−499.
(147) Becke, A. D. Density-Functional Thermochemistry. III. The Role of Exact Exchange. *J. Chem. Phys.* **1993**, *98* (7), 5648−5652.
(148) Lee, C.; Yang, W.; Parr, R. G. Development of the Colle-Salvetti Correlation-Energy Formula into a Functional of the Electron Density. *Phys. Rev. B* **1988**, *37* (2), 785−789.
(149) Zhao, Y.; Truhlar, D. G. The M06 Suite of Density Functionals for Main Group Thermochemistry, Thermochemical Kinetics, Noncovalent Interactions, Excited States, and Transition Elements: Two New Functionals and Systematic Testing of Four M06-Class Functionals and 12 Other Function. *Theor. Chem. Acc.* **2008**, *120* (1−3), 215−241.
(150) Zhao, Y.; Schultz, N. E.; Truhlar, D. G. Design of Density Functionals by Combining the Method of Constraint Satisfaction with Parametrization for Thermochemistry, Thermochemical Kinetics, and Noncovalent Interactions. *J. Chem. Theory Comput.* **2006**, *2* (2), 364−382.
(151) Zhao, Y.; Truhlar, D. G. How Well Can New-Generation Density Functionals Describe the Energetics of Bond-Dissociation Reactions Producing Radicals? *J. Phys. Chem. A* **2008**, *112* (6), 1095−1099.
(152) De Souza, G. L. C.; Peterson, K. A. Benchmarking Antioxidant-Related Properties for Gallic Acid through the Use of DFT, MP2, CCSD, and CCSD(T) Approaches. *J. Phys. Chem. A* **2021**, *125* (1), 198−208.
(153) Spiegel, M.; Gamian, A.; Sroka, Z. A Statistically Supported Antioxidant Activity DFT Benchmark—The Effects of Hartree-Fock Exchange and Basis Set Selection on Accuracy and Resources Uptake. *Molecules* **2021**, *26* (16), 5058.
(154) Galano, A.; Mazzone, G.; Alvarez-Diduk, R.; Marino, T.; Alvarez-Idaboy, J. R.; Russo, N. Food Antioxidants: Chemical Insights at the Molecular Level. *Annu. Rev. Food Sci. Technol.* **2016**, *7* (1), 335−352.
(155) Wang, J.; Becke, A. D.; Smith, V. H. Evaluation of ⟨S2⟩ in Restricted, Unrestricted Hartree-Fock, and Density Functional Based Theories. *J. Chem. Phys.* **1995**, *102* (8), 3477−3480.
(156) Brovarets', O. O.; Hovorun, D. M. Conformational Diversity of the Quercetin Molecule: A Quantum-Chemical View. *J. Biomol. Struct. Dyn.* **2020**, *38* (10), 2817−2836.
(157) Scalmani, G.; Frisch, M. J. Continuous Surface Charge Polarizable Continuum Models of Solvation. I. General Formalism. *J. Chem. Phys.* **2010**, *132* (11), 114110.
(158) Barone, V.; Cossi, M. Quantum Calculation of Molecular Energies and Energy Gradients in Solution by a Conductor Solvent Model. *J. Phys. Chem. A* **1998**, *102* (11), 1995−2001.
(159) Cossi, M.; Rega, N.; Scalmani, G.; Barone, V. Energies, Structures, and Electronic Properties of Molecules in Solution with the C-PCM Solvation Model. *J. Comput. Chem.* **2003**, *24* (6), 669−681.
(160) Marenich, A. V.; Cramer, C. J.; Truhlar, D. G. Universal Solvation Model Based on Solute Electron Density and on a Continuum Model of the Solvent Defined by the Bulk Dielectric Constant and Atomic Surface Tensions. *J. Phys. Chem. B* **2009**, *113* (18), 6378−6396.
(161) Kelly, C. P.; Cramer, C. J.; Truhlar, D. G. Adding Explicit Solvent Molecules to Continuum Solvent Calculations for the Calculation of Aqueous Acid Dissociation Constants. *J. Phys. Chem. A* **2006**, *110* (7), 2493−2499.
(162) Okuno, Y. Theoretical Investigation of the Mechanism of the Baeyer-Villiger Reaction in Nonpolar Solvents. *Chem. - A Eur. J.* **1997**, *3* (2), 212−218.
(163) Benson, S. W. *The Foundation of Chemical Kinetics*; McGraw-Hill, 1960.
(164) Medina, M. E.; Iuga, C.; Alvarez-Idaboy, J. R. Antioxidant Activity of Propyl Gallate in Aqueous and Lipid Media: A Theoretical Study. *Phys. Chem. Chem. Phys.* **2013**, *15* (31), 13137.
(165) Brovarets', O. O.; Hovorun, D. M. Conformational Transitions of the Quercetin Molecule via the Rotations of Its Rings: A Comprehensive Theoretical Study. *J. Biomol. Struct. Dyn.* **2020**, *38* (10), 2865−2883.
(166) Allouche, A. Gabedit — A Graphical User Interface for Computational Chemistry Softwares. *J. Comput. Chem.* **2011**, *32*, 174−182.
(167) Hanwell, M. D; Curtis, D. E; Lonie, D. C; Vandermeersch, T.; Zurek, E.; Hutchison, G. R Avogadro: An Advanced Semantic Chemical Editor, Visualization, and Analysis Platform. *J. Cheminform.* **2012**, *4* (8), 17.
(168) O'Boyle, N. M.; Banck, M.; James, C. A.; Morley, C.; Vandermeersch, T.; Hutchison, G. R. Open Babel: An Open Chemical Toolbox. *J. Cheminform.* **2011**, *3* (1), 33.
(169) Van Der Spoel, D.; Lindahl, E.; Hess, B.; Groenhof, G.; Mark, A. E.; Berendsen, H. J. C. GROMACS: Fast, Flexible, and Free. *J. Comput. Chem.* **2005**, *26* (16), 1701−1718.
(170) Salomon-Ferrer, R.; Case, D. A.; Walker, R. C. An Overview of the Amber Biomolecular Simulation Package. *Wiley Interdiscip. Rev. Comput. Mol. Sci.* **2013**, *3* (2), 198−210.
(171) Brooks, B. R.; Brooks, C. L.; Mackerell, A. D.; Nilsson, L.; Petrella, R. J.; Roux, B.; Won, Y.; Archontis, G.; Bartels, C.; Boresch, S.; Caflisch, A.; Caves, L.; Cui, Q.; Dinner, A. R.; Feig, M.; Fischer, S.; Gao, J.; Hodoscek, M.; Im, W.; Kuczera, K.; Lazaridis, T.; Ma, J.; Ovchinnikov, V.; Paci, E.; Pastor, R. W.; Post, C. B.; Pu, J. Z.; Schaefer, M.; Tidor, B.; Venable, R. M.; Woodcock, H. L.; Wu, X.; Yang, W.; York, D. M.; Karplus, M. CHARMM: The Biomolecular Simulation Program. *J. Comput. Chem.* **2009**, *30* (10), 1545−1614.
(172) Jo, S.; Kim, T.; Iyer, V. G.; Im, W. CHARMM-GUI: A Web-Based Graphical User Interface for CHARMM. *J. Comput. Chem.* **2008**, *29* (11), 1859−1865.
(173) Malde, A. K.; Zuo, L.; Breeze, M.; Stroet, M.; Poger, D.; Nair, P. C.; Oostenbrink, C.; Mark, A. E. An Automated Force Field Topology Builder (ATB) and Repository: Version 1.0. *J. Chem. Theory Comput.* **2011**, *7* (12), 4026−4037.
(174) Vanommeslaeghe, K.; MacKerell, A. D. Automation of the CHARMM General Force Field (CGenFF) I: Bond Perception and Atom Typing. *J. Chem. Inf. Model.* **2012**, *52* (12), 3144−3154.
(175) Daura, X.; Gademann, K.; Jaun, B.; Seebach, D.; van Gunsteren, W. F.; Mark, A. E. Peptide Folding: When Simulation Meets Experiment. *Angew. Chemie Int. Ed.* **1999**, *38* (1−2), 236−240.
(176) Ho, J.; Coote, M. L. A Universal Approach for Continuum Solvent PK a Calculations: Are We There Yet? *Theor. Chem. Acc.* **2010**, *125* (1−2), 3−21.
(177) Casasnovas, R.; Ortega-Castro, J.; Frau, J.; Donoso, J.; Muñoz, F. Theoretical PKa Calculations with Continuum Model Solvents, Alternative Protocols to Thermodynamic Cycles. *Int. J. Quantum Chem.* **2014**, *114* (20), 1350−1363.
(178) Tošović, J.; Marković, S.; Milenković, D.; Marković, Z. Solvation Enthalpies and Gibbs Energies of the Proton and Electron - Influence of Solvation Models. *J. Serbian Soc. Comput. Mech.* **2016**, *10* (2), 66−76.
(179) Malloum, A.; Fifen, J. J.; Conradie, J. Determination of the Absolute Solvation Free Energy and Enthalpy of the Proton in Solutions. *J. Mol. Liq.* **2021**, *322*, 114919.
(180) Marković, Z.; Milenković, D.; Dorović, J.; Jeremić, S. Solvation Enthalpies of the Proton and Electron in Polar and Non-Polar Solvents. *J. Serbian Soc. Comput. Mech.* **2013**, *7* (2), 1−9.
(181) Marković, Z.; Tošović, J.; Milenković, D.; Marković, S. Revisiting the Solvation Enthalpies and Free Energies of the Proton and Electron in Various Solvents. *Comput. Theor. Chem.* **2016**, *1077*, 11−17.
(182) Galano, A.; Pérez-González, A.; Castañeda-Arriaga, R.; Muñoz-Rugeles, L.; Mendoza-Sarmiento, G.; Romero-Silva, A.; Ibarra-Escutia, A.; Rebollar-Zepeda, A. M.; León-Carmona, J. R.; Hernández-Olivares, M. A.; Alvarez-Idaboy, J. R. Empirically Fitted Parameters for

https://doi.org/10.1021/acs.jcim.2c00104
J. Chem. Inf. Model. 2022, 62, 2639−2658

Calculating PKa Values with Small Deviations from Experiments Using a Simple Computational Strategy. *J. Chem. Inf. Model.* **2016**, *56* (9), 1714−1724.
(183) Pérez-González, A.; Castañeda-Arriaga, R.; Verastegui, B.; Carreón-González, M.; Alvarez-Idaboy, J. R.; Galano, A. Estimation of Empirically Fitted Parameters for Calculating PK a Values of Thiols in a Fast and Reliable Way. *Theor. Chem. Acc.* **2018**, *137* (1), 5.
(184) Rossini, E.; Bochevarov, A. D.; Knapp, E. W. Empirical Conversion of p K a Values between Different Solvents and Interpretation of the Parameters: Application to Water, Acetonitrile, Dimethyl Sulfoxide, and Methanol. *ACS Omega* **2018**, *3* (2), 1653−1662.
(185) Gramatica, P. Principles of QSAR Modeling. *Int. J. Quant. Struct. Relationships* **2020**, *5* (3), 61−97.
(186) Fukui, K.; Yonezawa, T.; Shingu, H. A Molecular Orbital Theory of Reactivity in Aromatic Hydrocarbons. *J. Chem. Phys.* **1952**, *20* (4), 722−725.
(187) Janak, J. F. Proof That ∂E∂ni = ε in Density-Functional Theory. *Phys. Rev. B* **1978**, *18* (12), 7165−7168.
(188) Koopmans, T. Über Die Zuordnung von Wellenfunktionen Und Eigenwerten Zu Den Einzelnen Elektronen Eines Atoms. *Physica* **1934**, *1* (1−6), 104−113.
(189) Parr, R. G.; Szentpály, L. v.; Liu, S. Electrophilicity Index. *J. Am. Chem. Soc.* **1999**, *121* (9), 1922−1924.
(190) Ortiz, J. V. Electron Propagator Theory: An Approach to Prediction and Interpretation in Quantum Chemistry. *Wiley Interdiscip. Rev. Comput. Mol. Sci.* **2013**, *3* (2), 123−142.
(191) Ortiz, J. V. Partial Third-order Quasiparticle Theory: Comparisons for Closed-shell Ionization Energies and an Application to the Borazine Photoelectron Spectrum. *J. Chem. Phys.* **1996**, *104* (19), 7599−7605.
(192) Pérez-González, A.; Galano, A.; Ortiz, J. V. Vertical Ionization Energies of Free Radicals and Electron Detachment Energies of Their Anions: A Comparison of Direct and Indirect Methods Versus Experiment. *J. Phys. Chem. A* **2014**, *118* (31), 6125−6131.
(193) Ortiz, J. V. Quasiparticle Approximations and Electron Propagator Theory. *Int. J. Quantum Chem.* **2003**, *95* (4−5), 593−599.
(194) Singh, R. K.; Ortiz, J. V.; Mishra, M. K. Tautomeric Forms of Adenine: Vertical Ionization Energies and Dyson Orbitals. *Int. J. Quantum Chem.* **2009**, na.
(195) Martínez, A.; Rodríguez-Girones, M. A.; Barbosa, A.; Costas, M. Donator Acceptor Map for Carotenoids, Melatonin and Vitamins. *J. Phys. Chem. A* **2008**, *112* (38), 9037−9042.
(196) Gázquez, J. L.; Cedillo, A.; Vela, A. Electrodonating and Electroaccepting Powers. *J. Phys. Chem. A* **2007**, *111* (10), 1966−1970.
(197) Gazquez, J. L. Perspectives on the Density Functional Theory of Chemical Reactivity. *J. Mex. Chem. Soc.* **2008**, *52* (1), 3−10.
(198) Martínez, A.; Vargas, R.; Galano, A. What Is Important to Prevent Oxidative Stress? A Theoretical Study on Electron-Transfer Reactions between Carotenoids and Free Radicals. *J. Phys. Chem. B* **2009**, *113* (35), 12113−12120.
(199) Parr, R. G.; Yang, W. Density Functional Approach to the Frontier-Electron Theory of Chemical Reactivity. *J. Am. Chem. Soc.* **1984**, *106* (14), 4049−4050.
(200) Mei, Y.; Simmonett, A. C.; Pickard, F. C.; Distasio, R. A.; Brooks, B. R.; Shao, Y. Numerical Study on the Partitioning of the Molecular Polarizability into Fluctuating Charge and Induced Atomic Dipole Contributions. *J. Phys. Chem. A* **2015**, *119* (22), 5865−5882.
(201) Martin, F.; Zipse, H. Charge Distribution in the Water Molecule -A Comparison of Methods. *J. Comput. Chem.* **2005**, *26* (1), 97−105.
(202) Mao, J. X. Atomic Charges in Molecules: A Classical Concept in Modern Computational Chemistry. *Postdoc J.* **2014**, *2* (2), na DOI: 10.14304/SURYA.JPR.V2N2.2.
(203) Bultinck, P.; Carbó-Dorca, R.; Langenaeker, W. Negative Fukui Functions: New Insights Based on Electronegativity Equalization. *J. Chem. Phys.* **2003**, *118* (10), 4349−4356.
(204) Senthilkumar, L.; Kolandaivel, P. Study of Effective Hardness and Condensed Fukui Functions Using AIM, Ab Initio, and DFT Methods. *Mol. Phys.* **2005**, *103* (4), 547−556.
(205) De Proft, F.; Martin, J. M. L.; Geerlings, P. Calculation of Molecular Electrostatic Potentials and Fukui Functions Using Density Functional Methods. *Chem. Phys. Lett.* **1996**, *256* (4−5), 400−408.
(206) Martínez-Araya, J. I. Why Is the Dual Descriptor a More Accurate Local Reactivity Descriptor than Fukui Functions? *J. Math. Chem.* **2015**, *53* (2), 451−465.
(207) Kohen, R.; Gati, I. Skin Low Molecular Weight Antioxidants and Their Role in Aging and in Oxidative Stress. *Toxicology* **2000**, *148* (2−3), 149−157.
(208) Bader, R. F. W. Atoms in Molecules. *Acc. Chem. Res.* **1985**, *18* (1), 9−15.
(209) Bader, R. F. W. A Quantum Theory of Molecular Structure and Its Applications. *Chem. Rev.* **1991**, *91* (5), 893−928.
(210) Lu, T.; Chen, F. Multiwfn: A Multifunctional Wavefunction Analyzer. *J. Comput. Chem.* **2012**, *33* (5), 580−592.
(211) Jenkins, S.; Liu, Z.; Kirk, S. R. A Bond, Ring and Cage Resolved Poincaré-Hopf Relationship for Isomerisation Reaction Pathways. *Mol. Phys.* **2013**, *111* (20), 3104−3116.
(212) Pakiari, A. H.; Eskandari, K. The Chemical Nature of Very Strong Hydrogen Bonds in Some Categories of Compounds. *J. Mol. Struct. THEOCHEM* **2006**, *759* (1−3), 51−60.
(213) Shainyan, B. A.; Chipanina, N. N.; Aksamentova, T. N.; Oznobikhina, L. P.; Rosentsveig, G. N.; Rosentsveig, I. B. Intramolecular Hydrogen Bonds in the Sulfonamide Derivatives of Oxamide, Dithiooxamide, and Biuret. FT-IR and DFT Study, AIM and NBO Analysis. *Tetrahedron* **2010**, *66* (44), 8551−8556.
(214) Hibbs, D. E.; Overgaard, J.; Piltz, R. O. X-N Charge Density Analysis of the Hydrogen Bonding Motif in 1-(2-Hydroxy-5-Nitrophenyl)EthanoneElectronic Supplementary Information (ESI) Available: Multipole Population Coefficients and Pseudoatom Parameterization. See Http://Www.Rsc.Org/Suppdata/Ob/B2/. *Org. Biomol. Chem.* **2003**, *1* (7), 1191−1198.
(215) Popelier, P. L. A. Characterization of a Dihydrogen Bond on the Basis of the Electron Density. *J. Phys. Chem. A* **1998**, *102* (10), 1873−1878.
(216) Koch, U.; Popelier, P. L. A. Characterization of C-H-O Hydrogen Bonds on the Basis of the Charge Density. *J. Phys. Chem.* **1995**, *99* (24), 9747−9754.
(217) Ebrahimi, A.; Roohi, H.; Habibi, M.; Mohammadi, M.; Vaziri, R. Characterization of Conformers of Non-Ionized Proline on the Basis of Topological and NBO Analyses: Can Nitrogen Be a Donor of Hydrogen Bond? *Chem. Phys.* **2006**, *322* (3), 289−297.
(218) Rozas, I.; Alkorta, I.; Elguero, J. Behavior of Ylides Containing N, O, and C Atoms as Hydrogen Bond Acceptors. *J. Am. Chem. Soc.* **2000**, *122* (45), 11154−11161.
(219) Espinosa, E.; Molins, E.; Lecomte, C. Hydrogen Bond Strengths Revealed by Topological Analyses of Experimentally Observed Electron Densities. *Chem. Phys. Lett.* **1998**, *285* (3−4), 170−173.
(220) Mata, I.; Alkorta, I.; Espinosa, E.; Molins, E. Relationships between Interaction Energy, Intermolecular Distance and Electron Density Properties in Hydrogen Bonded Complexes under External Electric Fields. *Chem. Phys. Lett.* **2011**, *507* (1−3), 185−189.
(221) Korth, H. G.; De Heer, M. I.; Mulder, P. A DFT Study on Intramolecular Hydrogen Bonding in 2-Substituted Phenols: Conformations, Enthalpies, and Correlation with Solute Parameters. *J. Phys. Chem. A* **2002**, *106* (37), 8779−8789.
(222) Tognetti, V.; Joubert, L. On the Influence of Density Functional Approximations on Some Local Baders Atoms-in-Molecules Properties. *J. Phys. Chem. A* **2011**, *115* (21), 5505−5515.
(223) Jabłoński, M. QTAIM-Based Comparison of Agostic Bonds and Intramolecular Charge-Inverted Hydrogen Bonds. *J. Phys. Chem. A* **2015**, *119* (20), 4993−5008.
(224) Jabłoński, M.; Palusiak, M. Basis Set and Method Dependence in Quantum Theory of Atoms in Molecules Calculations for Covalent Bonds. *J. Phys. Chem. A* **2010**, *114* (47), 12498−12505.
(225) Foster, J. P.; Weinhold, F. Natural Hybrid Orbitals. *J. Am. Chem. Soc.* **1980**, *102* (24), 7211−7218.

(226) Reed, A. E.; Curtiss, L. A.; Weinhold, F. Intermolecular Interactions from a Natural Bond Orbital, Donor—Acceptor Viewpoint. *Chem. Rev.* **1988**, *88* (6), 899−926.
(227) Reed, A. E.; Weinstock, R. B.; Weinhold, F. Natural Population Analysis. *J. Chem. Phys.* **1985**, *83* (2), 735−746.
(228) Carpenter, J. E.; Weinhold, F. Analysis of the Geometry of the Hydroxymethyl Radical by the "Different Hybrids for Different Spins" Natural Bond Orbital Procedure. *J. Mol. Struct. THEOCHEM* **1988**, *169* (C), 41−62.
(229) Benassi, E.; Fan, H. Quantitative Characterisation of the Ring Normal Modes. Pyridine as a Study Case. *Spectrochim. Acta - Part A Mol. Biomol. Spectrosc.* **2021**, *246*, 119026.
(230) Rose, R. C.; Bode, A. M. Biology of Free Radical Scavengers: An Evaluation of Ascorbate. *FASEB J.* **1993**, *7* (12), 1135−1142.
(231) Galano, A.; Tan, D. X.; Reiter, R. J. Melatonin as a Natural Ally against Oxidative Stress: A Physicochemical Examination. *J. Pineal Res.* **2011**, *51* (1), 1−16.
(232) Márquez, L.; García-Bueno, B.; Madrigal, J. L. M.; Leza, J. C. Mangiferin Decreases Inflammation and Oxidative Damage in Rat Brain after Stress. *Eur. J. Nutr.* **2012**, *51* (6), 729−739.
(233) Masuda, T.; Yamada, K.; Maekawa, T.; Takeda, Y.; Yamaguchi, H. Antioxidant Mechanism Studies on Ferulic Acid: Identification of Oxidative Coupling Products from Methyl Ferulate and Linoleate. *J. Agric. Food Chem.* **2006**, *54* (16), 6069−6074.
(234) MASUDA, T.; YAMADA, K.; MAEKAWA, T.; TAKEDA, Y.; YAMAGUCHI, H. Antioxidant Mechanism Studies on Ferulic Acid: Isolation and Structure Identification of the Main Antioxidation Product from Methyl Ferulate. *Food Sci. Technol. Res.* **2006**, *12* (3), 173−177.
(235) Sies, H. Oxidative Stress: Oxidants and Antioxidants. *Exp. Physiol.* **1997**, *82* (2), 291−295.
(236) Terpinc, P.; Abramovič, H. A Kinetic Approach for Evaluation of the Antioxidant Activity of Selected Phenolic Acids. *Food Chem.* **2010**, *121* (2), 366−371.
(237) Land, E. J.; Ebert, M. *Trans. Faraday Soc.* **1967**, *63*, 1181.
(238) Aruoma, O. I.; Murcia, A.; Butler, J.; Halliwell, B. Evaluation of the Antioxidant and Prooxidant Actions of Gallic Acid and Its Derivatives. *J. Agric. Food Chem.* **1993**, *41* (11), 1880−1885.
(239) Galano, A. On the Direct Scavenging Activity of Melatonin towards Hydroxyl and a Series of Peroxyl Radicals. *Phys. Chem. Chem. Phys.* **2011**, *13* (15), 7178.
(240) Litwinienko, G.; Ingold, K. U. Abnormal Solvent Effects on Hydrogen Atom Abstractions. 1. The Reactions of Phenols with 2,2-Diphenyl-1-Picrylhydrazyl (Dpph •) in Alcohols. *J. Org. Chem.* **2003**, *68* (9), 3433−3438.
(241) Litwinienko, G.; Ingold, K. U. Abnormal Solvent Effects on Hydrogen Atom Abstraction. 2. Resolution of the Curcumin Antioxidant Controversy. The Role of Sequential Proton Loss Electron Transfer. *J. Org. Chem.* **2004**, *69* (18), 5888−5896.
(242) Litwinienko, G.; Ingold, K. U. Abnormal Solvent Effects on Hydrogen Atom Abstraction. 3. Novel Kinetics in Sequential Proton Loss Electron Transfer Chemistry. *J. Org. Chem.* **2005**, *70* (22), 8982−8990.
(243) Litwinienko, G.; Ingold, K. U. Solvent Effects on the Rates and Mechanisms of Reaction of Phenols with Free Radicals. *Acc. Chem. Res.* **2007**, *40* (3), 222−230.
(244) Bartmess, J. E. Thermodynamics of the Electron and the Proton. *J. Phys. Chem.* **1994**, *98* (25), 6420−6424.
(245) Halliwell, B.; Murcia, M. A.; Chirico, S.; Aruoma, O. I. Free Radicals and Antioxidants in Food and in Vivo: What They Do and How They Work. *Crit. Rev. Food Sci. Nutr.* **1995**, *35* (1−2), 7−20.
(246) Halliwell, B.; Whiteman, M. Measuring Reactive Species and Oxidative Damage in Vivo and in Cell Culture: How Should You Do It and What Do the Results Mean? *Br. J. Pharmacol.* **2004**, *142* (2), 231−255.
(247) Bell, R. P. The Theory of Reactions Involving Proton Transfers. *Proc. R. Soc. London. Ser. A - Math. Phys. Sci.* **1936**, *154* (882), 414−429.
(248) Evans, M. G.; Polanyi, M. Further Considerations on the Thermodynamics of Chemical Equilibria and Reaction Rates. *Trans. Faraday Soc.* **1936**, *32*, 1333.
(249) Muraro, C.; Polato, M.; Bortoli, M.; Aiolli, F.; Orian, L. Radical scavenging activity of natural antioxidants and drugs: Development of a combined machine learning and quantum chemistry protocol. *J. Chem. Phys.* **2020**, *153*, 114117.
(250) Ribaudo, G.; Bortoli, M.; Witt, C. E.; Parke, B.; Mena, S.; Oselladore, E.; Zagotto, G.; Hashemi, P.; Orian, L. ROS-Scavenging Selenofluoxetine Derivatives Inhibit In Vivo Serotonin Reuptake. *ACS Omega* **2022**, *7*, 8314−8322.
(251) Ulstrup, J.; Jortner, J. The Effect of Intramolecular Quantum Modes on Free Energy Relationships for Electron Transfer Reactions. *J. Chem. Phys.* **1975**, *63* (10), 4358−4368.
(252) Marcus, R. A.; Sutin, N. Electron Transfers in Chemistry and Biology. *Biochim. Biophys. Acta - Rev. Bioenerg.* **1985**, *811* (3), 265−322.
(253) Marcus, R. A. Electron Transfer Reactions in Chemistry. Theory and Experiment. *Rev. Mod. Phys.* **1993**, *65* (3), 599−610.
(254) Marcus, R. A. Chemical and Electrochemical Electron-Transfer Theory. *Annu. Rev. Phys. Chem.* **1964**, *15* (1), 155−196.
(255) Marcus, R. A. On the Theory of Oxidation-Reduction Reactions Involving Electron Transfer. III. Applications to Data on the Rates of Organic Redox Reactions. *J. Chem. Phys.* **1957**, *26* (4), 872−877.
(256) Eyring, H. The Activated Complex in Chemical Reactions. *J. Chem. Phys.* **1935**, *3* (2), 107−115.
(257) Evans, M. G.; Polanyi, M. Some Applications of the Transition State Method to the Calculation of Reaction Velocities, Especially in Solution. *Trans. Faraday Soc.* **1935**, *31*, 875.
(258) Truhlar, D. G.; Garrett, B. C.; Klippenstein, S. J. Current Status of Transition-State Theory. *J. Phys. Chem.* **1996**, *100* (31), 12771−12800.
(259) Eckart, C. The Penetration of a Potential Barrier by Electrons. *Phys. Rev.* **1930**, *35* (11), 1303−1309.
(260) Kuppermann, A.; Truhlar, D. G. Exact Tunneling Calculations. *J. Am. Chem. Soc.* **1971**, *93* (8), 1840−1851.
(261) Dzib, E.; Cabellos, J. L.; Ortíz-Chi, F.; Pan, S.; Galano, A.; Merino, G. Eyringpy : A Program for Computing Rate Constants in the Gas Phase and in Solution. *Int. J. Quantum Chem.* **2019**, *119* (2), No. e25686.
(262) Pollak, E.; Pechukas, P. Symmetry Numbers, Not Statistical Factors, Should Be Used in Absolute Rate Theory and in Broensted Relations. *J. Am. Chem. Soc.* **1978**, *100* (10), 2984−2991.
(263) Collins, F. C.; Kimball, G. E. Diffusion-Controlled Reaction Rates. *J. Colloid Sci.* **1949**, *4* (4), 425−437.
(264) Smoluchowski, M. v. Versuch Einer Mathematischen Theorie Der Koagulationskinetik Kolloider Lösungen. *Zeitschrift für Phys. Chemie* **1918**, *92U* (1), 129−168.
(265) Einstein, A. Über Die von Der Molekularkinetischen Theorie Der Wärme Geforderte Bewegung von in Ruhenden Flüssigkeiten Suspendierten Teilchen. *Ann. Phys.* **1905**, *322* (8), 549−560.
(266) Galano, A.; Alvarez-Idaboy, J. R. A Computational Methodology for Accurate Predictions of Rate Constants in Solution: Application to the Assessment of Primary Antioxidant Activity. *J. Comput. Chem.* **2013**, *34* (28), 2430−2445.
(267) Olson, K. R. Reactive Oxygen Species or Reactive Sulfur Species: Why We Should Consider the Latter. *J. Exp. Biol.* **2020**, *223* (4), jeb196352.
(268) Dedon, P. C.; Tannenbaum, S. R. Reactive Nitrogen Species in the Chemical Biology of Inflammation. *Arch. Biochem. Biophys.* **2004**, *423* (1), 12−22.
(269) Reinke, L. A. Spin Trapping Evidence for Alcohol-Associated Oxidative Stress1,2 1This Article Is Part of a Series of Reviews on "Alcohol, Oxidative Stress, and Cell Injury." The Full List of Papers May Be Found on the Homepage of the Journal. *Free Radic. Biol. Med.* **2002**, *32* (10), 953−957.

https://doi.org/10.1021/acs.jcim.2c00104
J. Chem. Inf. Model. 2022, 62, 2639−2658